https://doi.org/10.1093/plcell/koac046 THE PLANT CELL 2022: 34: 1844–1862

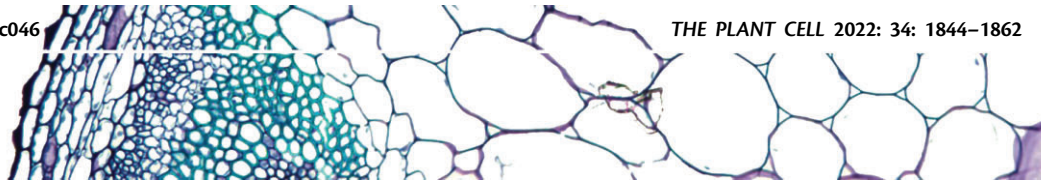

Research Article

Nitrate transport via NRT2.1 mediates NIN-LIKE PROTEIN-dependent suppression of root nodulation in *Lotus japonicus*

Fumika Misawa [1], Momoyo Ito [1], Shohei Nosaki [1,2], Hanna Nishida [3], Masahiro Watanabe [1], Takamasa Suzuki [4], Kenji Miura [1,2], Masayoshi Kawaguchi [5,6] and Takuya Suzaki [1,2,*,†]

1 Faculty of Life and Environmental Sciences, University of Tsukuba, Tsukuba, Ibaraki, Japan
2 Tsukuba Plant-Innovation Research Center, University of Tsukuba, Tsukuba, Ibaraki, Japan
3 Institute of Agrobiological Sciences, National Agriculture and Food Research Organization, Tsukuba, Ibaraki, Japan
4 College of Bioscience and Biotechnology, Chubu University, Kasugai, Aichi, Japan
5 National Institute for Basic Biology, Okazaki, Aichi, Japan
6 School of Life Science, Graduate University for Advanced Studies, Okazaki, Aichi, Japan

*Author for correspondence: suzaki.takuya.fn@u.tsukuba.ac.jp
†Senior author.
These authors contributed equally (F.M. and M.I.).
T.Suza. conceived the project. F.M., M.I., H.N., M.K., and T.Suza. designed the experiments. F.M., M.I., S.N., H.N., M.W., K.M., T.Suzu., and T.Suza. performed experiments and analyzed the data. T.Suza. wrote the manuscript, which was approved by all authors.
The author responsible for distribution of materials integral to the findings presented in this article in accordance with the policy described in the Instructions for Authors (https://academic.oup.com/plcell) is: Takuya Suzaki (suzaki.takuya.fn@u.tsukuba.ac.jp).

Abstract

Legumes have adaptive mechanisms that regulate nodulation in response to the amount of nitrogen in the soil. In *Lotus japonicus*, two NODULE INCEPTION (NIN)-LIKE PROTEIN (NLP) transcription factors, LjNLP4 and LjNLP1, play pivotal roles in the negative regulation of nodulation by controlling the expression of symbiotic genes in high nitrate conditions. Despite an improved understanding of the molecular basis for regulating nodulation, how nitrate plays a role in the signaling pathway to negatively regulate this process is largely unknown. Here, we show that nitrate transport via NITRATE TRANSPORTER 2.1 (LjNRT2.1) is a key step in the NLP signaling pathway to control nodulation. A mutation in the *LjNRT2.1* gene attenuates the nitrate-induced control of nodulation. LjNLP1 is necessary and sufficient to induce *LjNRT2.1* expression, thereby regulating nitrate uptake/transport. Our data suggest that LjNRT2.1-mediated nitrate uptake/transport is required for LjNLP4 nuclear localization and induction/repression of symbiotic genes. We further show that LjNIN, a positive regulator of nodulation, counteracts the LjNLP1-dependent induction of *LjNRT2.1* expression, which is linked to a reduction in nitrate uptake. These findings suggest a plant strategy in which nitrogen acquisition switches from obtaining nitrogen from the soil to symbiotic nitrogen fixation.

Introduction

Nitrogen acquisition is critical for plant growth. Growth of most plant species depends on water-soluble forms of nitrogen nutrients such as nitrate and ammonia in the soil (Oldroyd and Leyser, 2020). Legumes can establish endosymbiotic relationships with nitrogen-fixing bacteria called rhizobia by forming root nodules; the rhizobia in the nodules fix

Received June 29, 2021. Accepted February 01, 2022. Advance access publication February 11, 2022

IN A NUTSHELL

Background: Through symbiosis with nitrogen-fixing bacteria, legumes can use nitrogen from the atmosphere as a nutrient. However, root nodule symbiosis requires energy and plants save energy when they can. For example, plants temporarily halt root nodule symbiosis when the soil contains an abundance of nitrogen-containing nutrients such as nitrate. In other words, plants have a mechanism to control root nodule symbiosis upon changes in the amount of nitrate. Using the model legume *Lotus japonicus*, we previously identified the NIN-LIKE PROTEINs LjNLP1 and LjNLP4 as key transcription factors that play pivotal roles in this regulation. However, how nitrate acts in the signalling pathway to control nodulation remains largely unknown.

Question: How do legume nitrate transporters control root nodule symbiosis in a nitrate-rich environment?

Findings: By analyzing mutants involved in the nitrate-mediated control of root nodule symbiosis, we showed that a defect in the nitrate transporter gene *LjNRT2.1* results in the maintenance of nodulation in nitrate-rich environments. We also found that LjNLP1 directly regulated *LjNRT2.1* expression. Furthermore, our data suggest that LjNRT2.1-mediated nitrate influx into the cell is relevant to nuclear localization of LjNLP4 and subsequent regulation of the expression of nodulation-related genes. Interestingly, LjNIN, a nodulation-specific transcription factor, controls nitrate uptake by interfering with *LjNRT2.1* expression by LjNLP1. These findings enhance our understanding of the mechanisms of nitrogen acquisition that is unique to nodulating plants.

Next steps: In plant evolution, legumes that depend on nodules for their nitrogen source may have developed a unique mode of nitrogen acquisition. Comparative functional analysis of nitrate transporter genes, including *NRT2.1*, in various plants may be useful in testing this hypothesis.

atmospheric nitrogen, thus making it available to plants (Oldroyd et al., 2011; Roy et al., 2020). Root nodule symbiosis plays an important role in the growth and survival of symbiotic host plants in a nitrogen-deficient environment. This symbiosis, however, is not always beneficial for plants because photosynthetic products that could be used for plant growth need to be consumed as energy sources for nodule development and nitrogen fixation. To maintain a balance between gaining nitrogen and losing carbon during root nodule symbiosis, plants control root nodule symbiosis depending on nitrogen nutrient availability in the soil (Nishida and Suzaki, 2018a); in nitrate-sufficient conditions, plants negatively regulate several key processes in root nodule symbiosis, including rhizobial infection, nodule initiation and growth, and the nitrogen fixation process (Streeter and Wong, 1988; Carroll and Mathews, 1990; Nishida and Suzaki, 2018b).

Soybean (*Glycine max*) *nitrate-tolerant symbiotic* (*nts*) mutants are the first identified legume mutants that affect nitrate-mediated control of nodulation (Carroll et al., 1985). In addition to their hypernodulating phenotypes, the *nts* mutants are tolerant to high nitrate concentrations. The gene responsible for the *nts-1* mutants encodes a shoot-acting receptor-like kinase, Nodule autoregulation receptor kinase (GmNARK; Searle et al., 2003). Defects in the *GmNARK* ortholog in two model legumes, *Lotus japonicus HYPERNODULATION ABERRANT ROOT FORMATION 1* (*LjHAR1*) and *Medicago truncatula SUPER NUMERIC NODULES*, exhibit similar phenotypes to the *Gmnark* mutants (Krusell et al., 2002; Nishimura et al., 2002; Schnabel et al., 2005). In addition, the expression of *CLAVATA3/ESR-related* (*CLE*)-*ROOT SIGNAL 2* (*LjCLE-RS2*), encoding a root-derived ligand of LjHAR1, is induced not only by rhizobial inoculation but also by nitrate treatment (Okamoto et al., 2009). In *M. truncatula*, rhizobia/nitrate-inducible *MtCLE35* was recently identified as a functional counterpart of *LjCLE-RS2* (Luo et al., 2021; Mens et al., 2021; Moreau et al., 2021). In nitrate-sufficient conditions, loss-of-function mutations in *LjHAR1* or *LjCLE-RS2* show tolerance to the nitrate-induced reduction in nodule number, not to other processes such as rhizobial infection and nodule growth (Nishida et al., 2018, 2020). These observations suggest the signaling pathway including these genes is responsible for modulating nodule number in the pleiotropic control of root nodule symbiosis by nitrate.

A recent genetic approach in *L. japonicus* identified *nitrate unresponsive symbiosis 1* (*nrsym1*) and *nrsym2* mutants that have a normal nodule number but attenuate nitrate-induced control of root nodule symbiosis (Nishida et al., 2018, 2021). *NRSYM1* and *NRSYM2* encode NODULE INCEPTION (NIN)-LIKE PROTEIN (NLP) transcription factor, LjNLP4 and LjNLP1, respectively. NLP is paralogous to NIN, a necessary and sufficient regulator of nodulation (Schauser et al., 1999, 2005; Soyano et al., 2013; Vernié et al., 2015). In addition to its positive role in nodulation, LjNIN/MtNIN negatively regulates nodulation via induction of *LjCLE-RS1/2* and *MtCLE13* (Soyano et al., 2014; Laffont et al., 2020). LjNLP4 shares common DNA-binding sites on the *LjCLE-RS2* promoter with LjNIN, and LjNLP4 negatively regulates nodule number by directly inducing *LjCLE-RS2* expression in response to nitrate (Nishida et al., 2018). Furthermore, the expression of LjNIN target genes with positive roles in rhizobial infection and nodule organogenesis are repressed by nitrate in LjNLP4- and LjNLP1-dependent manners (Nishida et al., 2021).

LjNLP4 localizes within nuclei in response to nitrate, as do the NLPs in other plants (Marchive et al., 2013; Liu et al., 2017; Lin et al., 2018; Nishida et al., 2018). Therefore, in the presence of high nitrate levels, nuclear-localized LjNLP4 can negatively regulate nodulation by bifunctional transcriptional regulation, inducing or repressing the expression of LjNIN target genes (Nishida et al., 2021). The induced genes include *LjCLE-RS2*, which has a negative role in nodulation, and the repressed genes include *NUCLEAR FACTOR Y-A* (*LjNF-YA*), *LjNF-YB*, *EXOPOLYSACCHARIDE RECEPTOR 3* (*LjEPR3*), and *RHIZOBIAL INFECTION RECEPTOR-LIKE KINASE 1*, which have positive roles in nodulation (Okamoto et al., 2009; Soyano et al., 2013; Kawaharada et al., 2015, 2017; Li et al., 2019; Shrestha et al., 2021). In *M. truncatula*, MtNLP1 directly induces *MtCLE35*, a negative regulator of nodulation, and represses *CYTOKININ RESPONSE 1*, a positive regulator of nodulation and a direct target of MtNIN (Lin et al., 2018; Luo et al., 2021). Hence, it is likely that the mode-of-action for NLP-mediated bifunctional transcriptional regulation of symbiotic genes is conserved in *L. japonicus* and *M. truncatula*.

Generally, plants use two different nitrate transport systems depending on the nitrate concentration: a high-affinity transport system (HATS) and a low-affinity transport system (LATS) for low (<0.5 mM) and high (>0.5 mM) nitrate concentration ranges, respectively (Krapp et al., 2014). In *Arabidopsis thaliana*, the NITRATE TRANSPORTER 2 (NRT2) family is primarily responsible for HATS, whereas the NRT1 family is responsible for LATS (Wang et al., 1998; Filleur et al., 2001; Li et al., 2007). An exception is AtNRT1.1, which can switch between high- and low-affinity transport activities depending on the phosphorylation state of the AtNRT1.1 protein (Ho et al., 2009). Several studies on legume nitrate transporters suggest their potential roles in nodulation and nitrate-induced control of nodulation (Pellizzaro et al., 2017). In particular, the roles of some *NITRATE PEPTIDE FAMILY* (*NPF*) genes have been characterized. MtNPF1.7 positively regulates nodulation and is dispensable for nitrate-induced control of nodulation (Yendrek et al., 2010). LjNPF8.6 is involved in nitrogen fixation (Valkov et al., 2017). In addition, the *Mtnpf7.6* mutants have nodules of reduced size and are tolerant to nitrate, suggesting that MtNPF7.6 is required for nodule growth and nitrate-induced control of nodulation (Wang et al., 2020).

Despite the accumulating examples of the roles of legume nitrate transporters, how the nitrate transport system plays a role in the signaling pathway to control nodulation under high nitrate conditions remains mostly elusive. This study shows that a mutation in *LjNRT2.1* maintains nodulation under high nitrate concentrations. Phenotypic analysis indicates that LjNRT2.1 and LjNLP1 act in the nitrate uptake/transport process. In addition, LjNLP1 is necessary and sufficient to induce *LjNRT2.1* expression, which is likely to be associated with the nitrate-dependent LjNLP4 nuclear localization and induction/repression of symbiotic genes. These data indicate that nitrate transport via LjNRT2.1 is a key process in the NLP signaling pathway to control nodulation. Furthermore, we show that LjNIN can counteract LjNLP1-dependent induction of *LjNRT2.1*. This mechanism may reflect a plant strategy in which the acquisition of nitrogen nutrients switches from depending on nitrogen in the soil to depending on symbiotic nitrogen fixation.

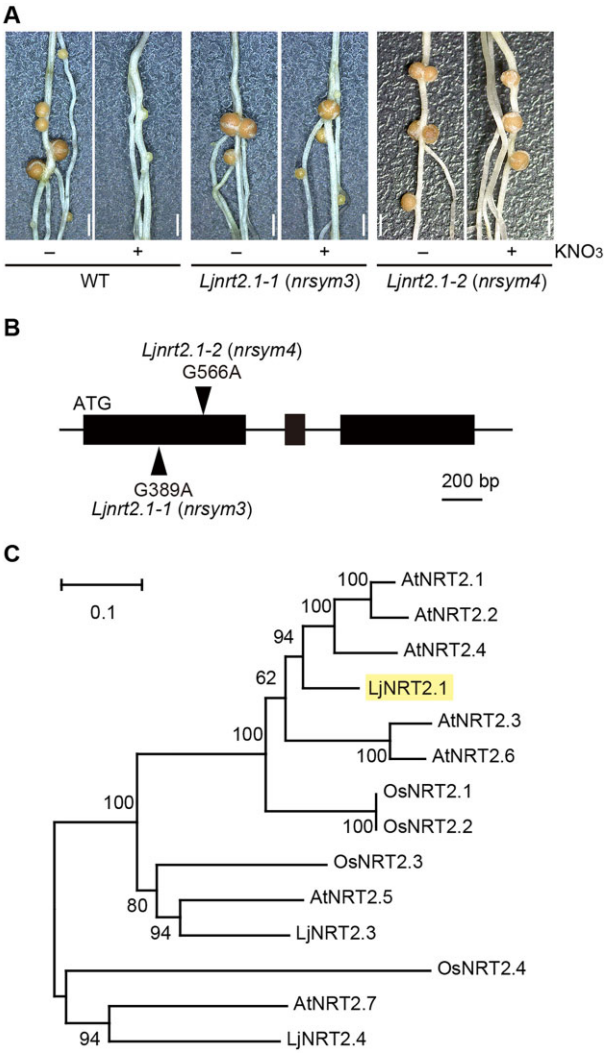

Figure 1 Identification of the *LjNRT2.1* gene. A, Nodule phenotypes of the WT, the *Ljnrt2.1-1*, and the *Ljnrt2.1-2* mutants grown with 0 (–) or 10 mM KNO_3 (+) for 21 dai. Scale bars = 1 mm. B, Exon-intron structure of the *LjNRT2.1* gene. The arrowheads indicate the locations of the *Ljnrt2.1-1* and the *Ljnrt2.1-2* mutations. C, A phylogenetic tree of the *NRT2* gene family from *A. thaliana*, *Oryza sativa*, and *L. japonicus* generated using the Neighbor-Joining method. The nomenclature for *LjNRT2* genes was based on previous studies (Criscuolo et al., 2012; Valkov et al., 2020). LjNRT2.2 was excluded from the phylogenetic tree, as this sequence is unlikely to be functional (Supplemental Figure S3). The percentage of replicate trees in which the associated taxa clustered together in the bootstrap test (1,000 replicates) are shown.

Results

LjNRT2.1 is required for nitrate-induced control of nodulation

In our previous screen for *L. japonicus* ethylmethane sulfonate (EMS) mutants involved in the nitrate response during nodulation (Nishida et al., 2018), we identified two new recessive mutants, *nrsym3* and *nrsym4*. Treatment with a high nitrate concentration (10 mM) attenuated nodulation in the wild-type (WT), but the effect of nitrate was suppressed by the *nrsym3* or the *nrsym4* mutations (Figure 1A). An allelism test suggested that the nitrate-unresponsive phenotypes of *nrsym3* and *nrsym4* were caused by a mutation in an identical gene, as F1 plants obtained from a cross between the plants formed mature nodules under high nitrate conditions (Supplemental Figure S1). A genome-resequencing approach using the *nrsym3* and *nrsym4* mutants identified a point mutation that caused a missense mutation in *LjNRT2.1* (Lj3g3v3069030; Criscuolo et al., 2012; Valkov et al., 2020), a gene that encodes a protein similar to Arabidopsis NRT2 proteins, including AtNRT2.1, AtNRT2.2, and AtNRT2.4 (Figure 1, B and C).

To test whether *LjNRT2.1* could complement the *nrsym3* mutant, a 6.4-kb genomic fragment, including the promoter (3.2 kb) and the terminator (1.2 kb) regions of *LjNRT2.1*, was introduced into the *nrsym3* mutants by *Agrobacterium rhizogenes*-mediated hairy root transformation. Nodulation on the mutant roots expressing the complementation construct was inhibited by nitrate (Supplemental Figure S2, A and B). This result indicates that Lj3g3v3069030 is responsible for the *nrsym3* mutation.

Hereafter, we unified the nomenclature by re-naming *nrsym3* and *nrsym4* as *Ljnrt2.1-1* and *Ljnrt2.1-2*, respectively. The typical structure of NRT2 family proteins has 12 transmembrane regions. Mutations in the *Ljnrt2.1-1* and *Ljnrt2.1-2* mutants are located in the third (G130D) and fifth (G189E) transmembrane regions, respectively. Previous studies showed that the *L. japonicus* genome has four genes in the *NRT2* family, including *LjNRT2.1*, *LjNRT2.2* (Lj3g3v3069010, Lj3g3v3069020, Lj3g3v3069040, Lj3g3v3069050), *LjNRT2.3* (Lj4g3v1085060), and *LjNRT2.4* (Lj1g3v3646440) (Criscuolo et al., 2012; Valkov et al., 2020). As the coding sequence (CDS) of *LjNRT2.2* available from the *L. japonicus* genome database seemed to be partial and possibly inaccurate, we determined the full-length CDS of *LjNRT2.2*. We found that the structure of *LjNRT2.2* in two WT ecotypes, MG-20 and Gifu, contains a premature stop codon, thus encoding a truncated version of protein relative to LjNRT2.1 (Supplemental Figure S3).

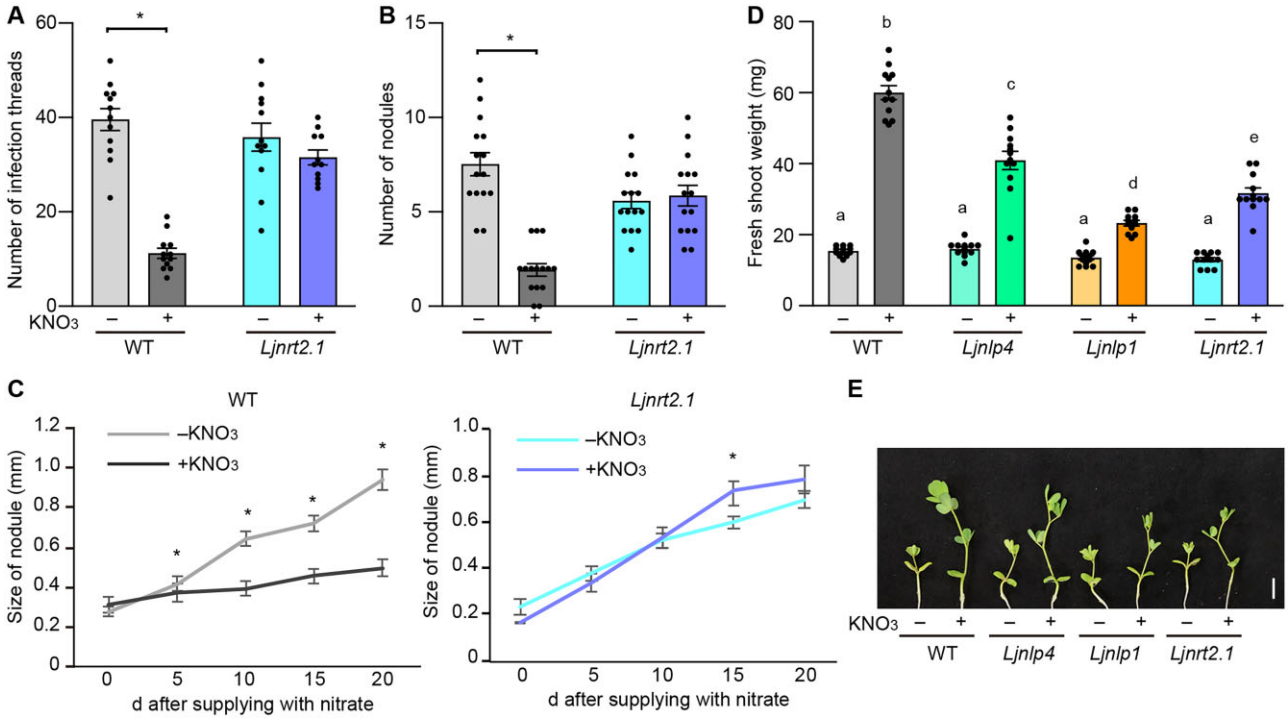

Figure 2 Nitrate effects on nodulation and plant growth in the *Ljnrt2.1* mutants. A–C, Nitrate effects on nodulation in the WT and *Ljnrt2.1-1* mutants. A, The number of infection threads in plants growing in 0 (–) or 10 mM KNO_3 (+) at 7 dai with rhizobia that constitutively express *DsRED* (n = 11–12 plants). B, The number of nodules in the presence of 0 (–) or 10 mM KNO_3 (+) for 21 dai (n = 15 plants). C, Nodule size of the WT and *Ljnrt2.1-1* mutants (n = 19–22 nodules). The WT and *Ljnrt2.1-1* plants were inoculated for 7 days in nitrate-free agar plates. After the formation of nodule primordia, the plants were transferred to new plates containing 0 or 10 mM KNO_3. Individual nodule size was measured at 0, 5, 10, 15, and 20 days after the transfer. Error bars indicate standard error of the mean (SEM). *$P < 0.05$ by a two-sided Welch's t test. D and E, Fresh shoot weight (D) and shoot growth (E) of the WT, *Ljnlp4-1*, *Ljnlp1*, and the *Ljnrt2.1-1* mutants grown in 0 (–) or 10 mM KNO_3 (+) in the absence of rhizobia for 13 days (n = 12 plants). Error bars indicate SEM. Different letters indicate statistically significant differences ($P < 0.05$, one-way analysis of variance (ANOVA) followed by multiple comparisons). Scale bar = 1 cm.

Therefore, it is likely that LjNRT2.2 is nonfunctional in some *L. japonicus* ecotypes.

Nitrate has pleiotropic effects on key events of nodulation, including rhizobial infection, nodule initiation, and nodule growth (Streeter and Wong, 1988; Carroll and Mathews, 1990; Nishida and Suzaki, 2018b). We, therefore, investigated whether the *Ljnrt2.1* mutation influenced these nitrate-affected nodulation processes. In the WT, the formation of infection threads, an indicator of rhizobial infection foci (Murray, 2011), was attenuated by nitrate; however, the nitrate-induced reduction in infection thread number was not observed in the *Ljnrt2.1* mutants (Figure 2A). In addition, the number of nodules formed on *Ljnrt2.1* roots in the presence of nitrate was comparable to that in the absence of nitrate (Figure 2B). Next, to focus on nodule growth, the WT and *Ljnrt2.1* plants were inoculated for 7 days in nitrate-free agar plates. After the formation of nodule primordia, the plants were transferred to new plates containing nitrate, and the successive changes in nodule size were measured. WT nodule growth was halted by nitrate, but the nitrate effect was largely abolished in the *Ljnrt2.1* mutants (Figure 2C). Therefore, these results indicate that LjNRT2.1 is required for nitrate-mediated control of rhizobial infection, nodule initiation, and growth.

The nodulation phenotypes of the *Ljnlp4* and the *Ljnlp1* mutants under high nitrate conditions are similar to those of the *Ljnrt2.1* mutants (Nishida et al., 2018, 2021). We then created multiple mutants and investigated the potential genetic relationships between the corresponding genes. Single, double, and triple mutants formed similar numbers of mature nodules that were indistinguishable from each other under high nitrate conditions (Supplemental Figure S4), suggesting that LjNLP4, LjNLP1, and LjNRT2.1 act in the same genetic pathway at least in the nitrate-induced control of nodulation.

We next tested the effect of nitrate on plant growth in the absence of rhizobia. Promotion of shoot growth by nitrate was diminished in each mutant relative to the WT, and the severity of the phenotype was strongest in *Ljnlp1*, weakest in *Ljnlp4*, and intermediate in *Ljnrt2.1* (Figure 2, D and E). The defect in nitrate-promoted shoot growth in the *Ljnrt2.1* plants was rescued by the introduction of a complementation construct (Supplemental Figure S2C), suggesting that LjNRT2.1 is responsible for the phenomenon.

LjNRT2.1 and LjNLP1 mediate nitrate uptake/transport

In WT, nitrate-induced inhibition of nodulation occurred in a dose-dependent manner: treatment with a high nitrate concentration (5 mM) reduced nodulation, whereas treatment with a low nitrate concentration (0.2 mM) did not affect nodulation (Figure 3, A and B; Nishida et al., 2018). The effect of nitrate (5 mM) was suppressed by the *Ljnrt2.1* mutations. As LjNRT2.1 belongs to the NRT2 family and *AtNRT2* genes are primarily responsible for HATS (Wang et al., 1998; Filleur et al., 2001; Li et al., 2007), we suspected that LjNRT2.1 might be involved in nitrate uptake/transport. To examine this possibility, the WT and *Ljnrt2.1* plants were treated with 0.2- or 5-mM nitrate solution that included a ^{15}N stable isotope in the presence of rhizobia, and the amount of ^{15}N in planta was measured. The nitrate uptake capacity in the root and shoot of the *Ljnrt2.1* mutants was significantly reduced compared with WT regardless of the exogenous nitrate concentration (Figure 3, C and D). In terms of nitrate uptake, noninoculated roots of the *Ljnrt2.1* mutants had a similar defect: the *Ljnrt2.1* mutations attenuated nitrate uptake in both low and high nitrate conditions (Supplemental Figure S5, A and B). These results suggest that LjNRT2.1 is required for nitrate uptake/transport.

We next analyzed the temporal changes in nitrate contents after nitrate treatment in noninoculated roots. Although the nitrate contents at relatively shorter time points (1 and 3 h) was unaffected in the *Ljnrt2.1* mutants, the reduction in nitrate contents become evident 6 h after nitrate treatment (10 mM; Figure 3E). Retarded shoot growth of the *Ljnlp4* and *Ljnlp1* mutants in the presence of nitrate implied that the mutants might be impaired in nitrate transport and/or utilization (Figure 2, D and E). We then investigated the nitrate contents 24 h after nitrate treatment (10 mM) in single, double, and triple mutants of *Ljnlp4*, *Ljnlp1*, and *Ljnrt2.1*. The nitrate contents were unaffected in the *Ljnlp4* mutants but were reduced in the *Ljnlp1* mutants to the same extent as in the *Ljnrt2.1* mutants (Figure 3F). The defect in nitrate uptake in the *Ljnlp1* mutants was also observed in the nitrate uptake assay using ^{15}N stable isotope (Supplemental Figure S5B). Therefore, these results suggest that LjNLP1 and LjNRT2.1 have roles in nitrate uptake/transport. LjNLP1 and LjNRT2.1 likely regulate nitrate uptake/transport in the same genetic pathway, as the nitrate contents in the *Ljnlp1 Ljnrt2.1* double mutants were equivalent to that of the *Ljnlp1* or the *Ljnrt2.1* single mutants. The relatively stronger defects in shoot growth in the *Ljnlp1* and the *Ljnrt2.1* mutants compared to the *Ljnlp4* mutants (Figure 2, D and E) were consistent with the defects in nitrate uptake in these mutants.

To verify the relationship between nitrate uptake/transport and gene expression, the expression of two nitrate-inducible genes, *NITRATE REDUCTASE* (*LjNIA*) and *LjCLE-RS2*, was analyzed in noninoculated roots by reverse transcription-quantitative polymerase chain reaction (RT-qPCR). Whereas the expression of *LjNIA* was rapidly (<0.5 h) induced, it took 6 h for the expression of *LjCLE-RS2* to be induced after nitrate treatment in the WT (Supplemental Figure S5, C and D). Transcript abundance of both genes was significantly reduced at later time points (>6 h) in the *Ljnrt2.1* mutants (Supplemental Figure S5, C and D), a result consistent with the observation that the *Ljnrt2.1* mutation attenuated nitrate uptake by 6 h and later (Figure 3E).

LjNLP1 is necessary and sufficient to induce *LjNRT2.1* expression in response to nitrate

We next analyzed the temporal expression pattern of *LjNRT2.1* in inoculated roots after nitrate treatment (10 mM) and the potential implications of LjNLP4 and

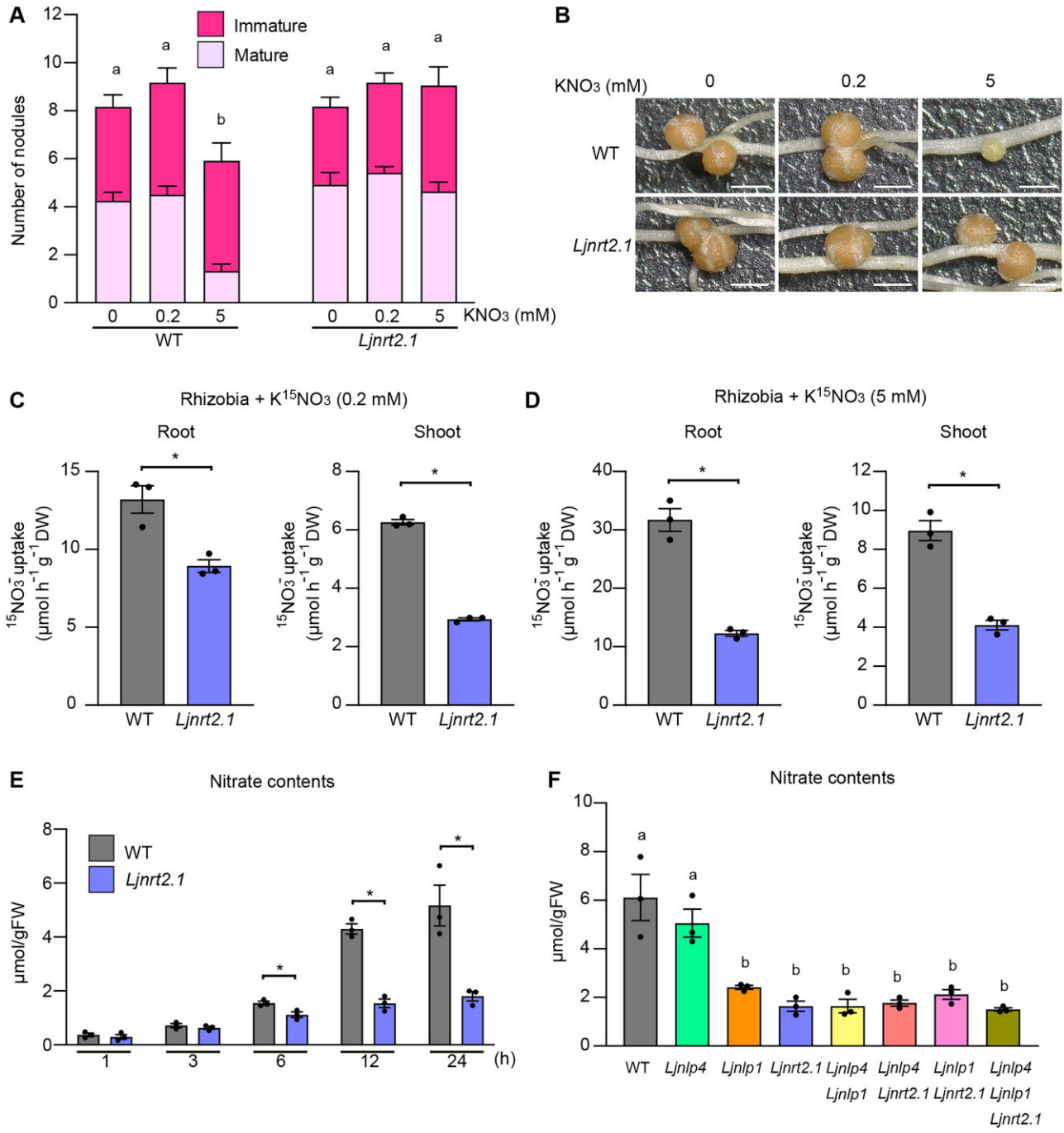

Figure 3 The capacity for nitrate uptake in the *Ljnrt2.1* mutants. A and B, Nodule number and nodulation phenotypes of the WT and *Ljnrt2.1-1* mutants in the presence of 0, 0.2, or 5 mM KNO_3 at 21 dai (n = 11–12 plants). Scale bars = 1 mm. C and D, The capacity for nitrate uptake by the WT and *Ljnrt2.1-1* mutants root and shoot in 0.2 (C) and 5 mM (D) KNO_3 in the presence of rhizobia. The plants were grown with 0.2 or 5 mM KNO_3 for 12 days in the presence of rhizobia. They were then treated with same concentration of $K^{15}NO_3$ for 24 h (n = 3 independent pools of roots derived from 12 plants). E, Temporal changes in the nitrate contents of noninoculated roots of the WT and *Ljnrt2.1-1* mutants after treatment with 10 mM KNO_3 (n = 3 independent pools of roots derived from seven plants). F, The nitrate contents of noninoculated roots of the WT and seven respective mutants 24 h after treatment with 10 mM KNO_3 (n = 3 independent pools of roots derived from seven plants). Error bars indicate SEM. *$P < 0.05$ by a two-sided Welch's t test (C–E). Different letters indicate statistically significant differences ($P < 0.05$, one-way ANOVA followed by multiple comparisons) (A) and (F).

LjNLP1 in *LjNRT2.1* expression. RT-qPCR analysis showed that, in the timescale tested, *LjNRT2.1* expression was inducible by nitrate treatment, and the expression level was highest at 3 h in the WT (Figure 4A). *LjNRT2.1* expression in the *Ljnlp4* mutants was largely comparable to that of the WT at least earlier time points (<3 h). At later time points (>24 h), the *LjNRT2.1* expression in the *Ljnlp4* mutants was constantly higher than WT. Of note, the *LjNRT2.1* expression

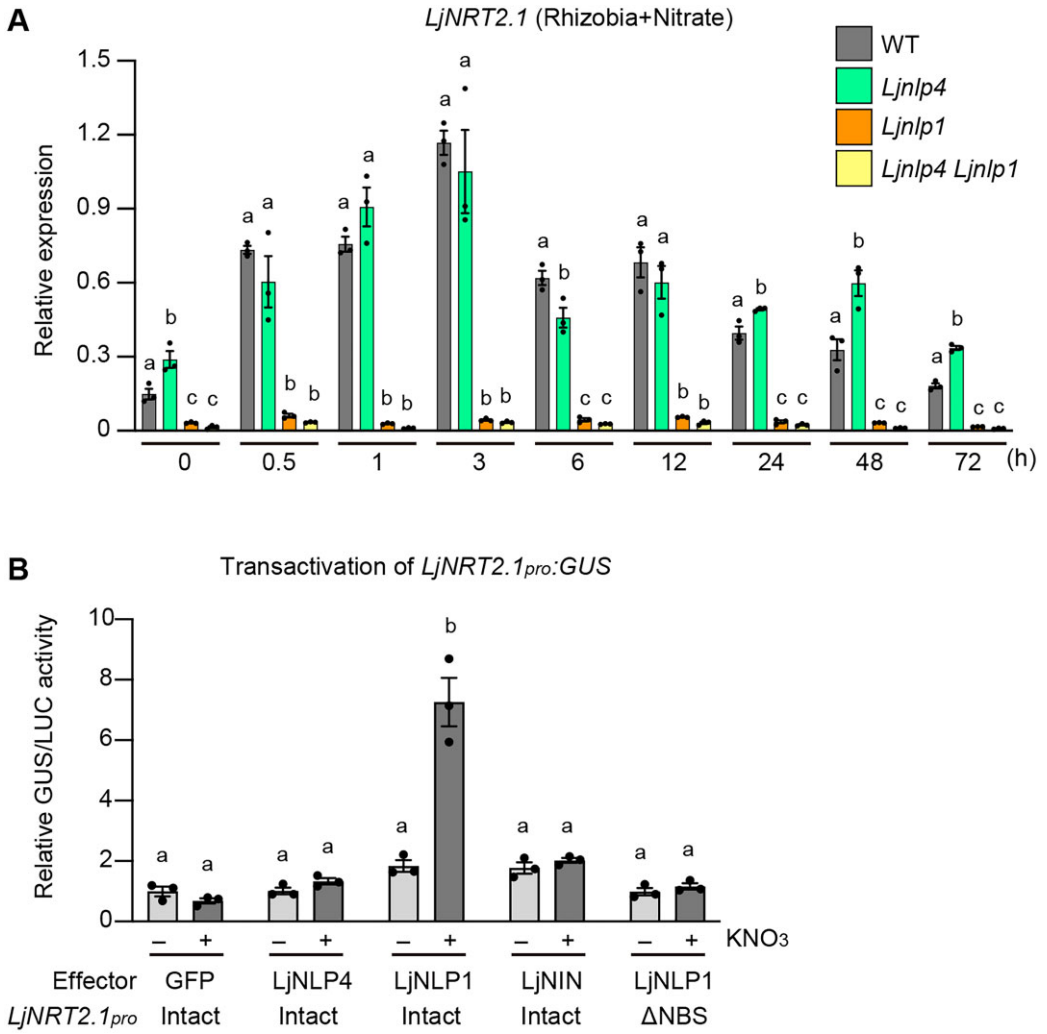

Figure 4 Temporal expression of *LjNRT2.1* and transactivation of *LjNRT2.1*. A, RT-qPCR analysis of temporal *LjNRT2.1* expression of the WT, *Ljnlp4-1*, *Ljnlp1*, and *Ljnlp4-1 Ljnlp1* mutants after simultaneous treatment with 10mM KNO_3 and rhizobia. Each cDNA sample was prepared from total RNA derived from inoculated roots treated with 10mM KNO_3 ($n = 3$ independent pools of roots derived from four plants). The expression of *LjUBQ* was used as the reference. Error bars indicate SEM. Different letters indicate statistically significant differences ($P < 0.05$, one-way ANOVA followed by multiple comparisons). Data for each time point were used in the statistical analysis. B, Transactivation of $LjNRT2.1_{pro}$:*GUS* in *L. japonicus* mesophyll protoplasts transformed with respective constructs ($n = 3$ independent pools of protoplasts). *GFP*, *LjNLP4*, *LjNLP1*, and *LjNIN* were used as effectors. Two types of $LjNRT2.1_{pro}$:*GUS* reporter constructs were used, one with an intact *LjNRT2.1* promoter and one with a modified *LjNRT2.1* promoter in which the NBS (Soyano et al., 2015) was specifically deleted (ΔNBS) (Supplemental Figure S6). Transformed protoplasts were incubated with 0 (−) or 10 mM (+) KNO_3. GUS activity was measured relative to $35S_{pro}$:*LUC* activity. Transactivation data were normalized to the condition in which *GFP* was expressed in the absence of KNO_3. Error bars indicate SEM. Different letters indicate statistically significant differences ($P < 0.05$, one-way ANOVA followed by multiple comparisons).

was abolished in the *Ljnlp1* mutants at every time point. The *LjNRT2.1* expression pattern in the *Ljnlp4 Ljnlp1* double mutants was indistinguishable from that of *Ljnlp1* (Figure 4A).

We next investigated whether LjNLP1 was sufficient to induce *LjNRT2.1* expression by a transactivation assay using mesophyll protoplasts of *L. japonicus*. Although LjNLP4 or LjNIN did not affect *LjNRT2.1* expression, LjNLP1 did induce *LjNRT2.1* expression in a nitrate-dependent manner (Figure 4B). The 3.2-kb $LjNRT2.1_{pro}$ region used in the transactivation assay had an LjNIN-binding sequence (NBS; Soyano et al., 2015). Given the similarity of the DNA-binding sites between NLP and NIN (Soyano et al., 2015; Nishida et al., 2021), we assumed that the NBS in the $LjNRT2.1_{pro}$ might be relevant to LjNLP1-mediated *LjNRT2.1* expression. LjNLP1 failed to express the *GUS* reporter gene under the control of a modified $LjNRT2.1_{pro}$ in which the NBS was specifically deleted (Figure 4B; Supplemental Figure S6A). Taken

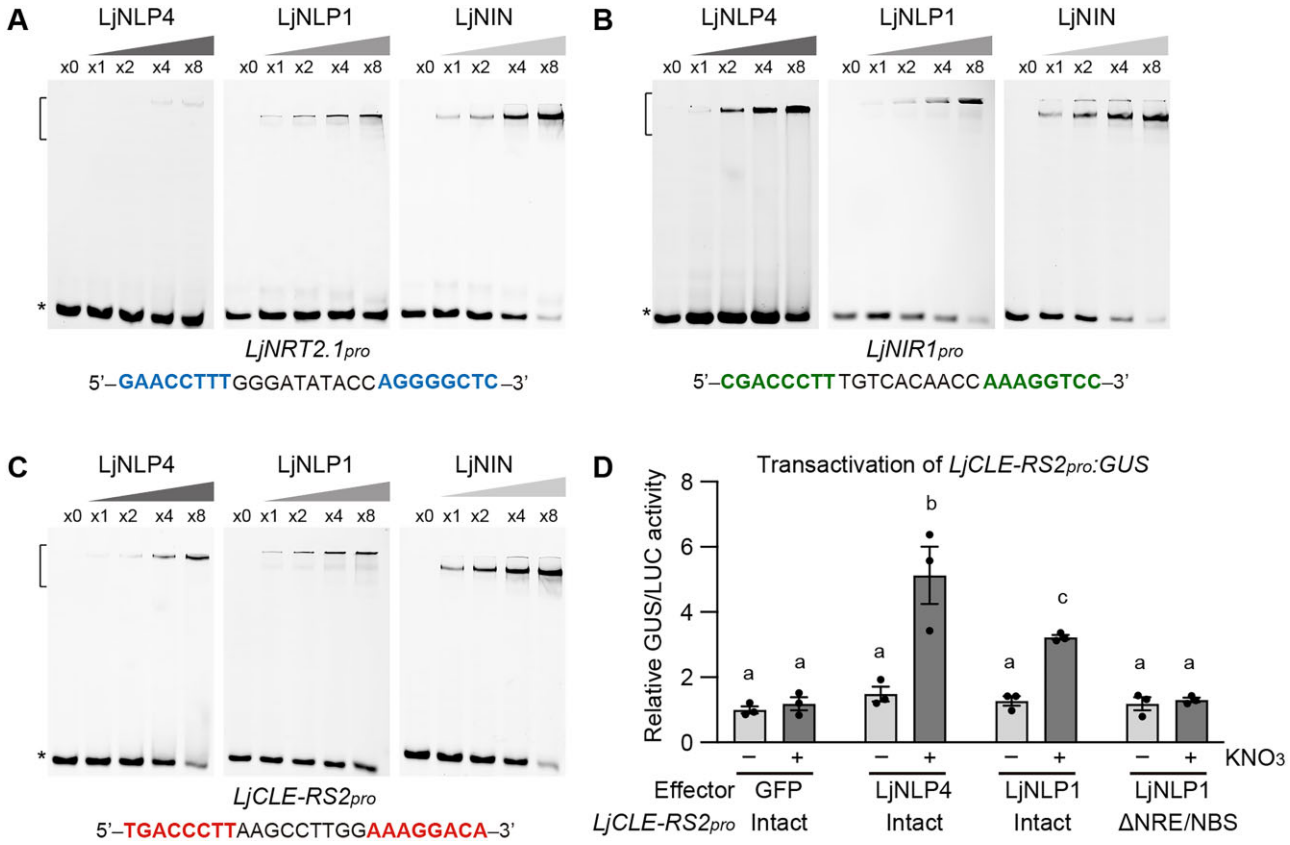

Figure 5 Protein–DNA interaction of LjNLP4, LjNLP1, and LjNIN. A–C, EMSA showing LjNLP4, LjNLP1, or LjNIN binding to the *cis*-elements on the *LjNRT2.1*$_{pro}$ (A), *LjNIR1*$_{pro}$ (B), and *LjCLE-RS2*$_{pro}$ (C). MBP-LjNLP4 (564–976), MBP-LjNLP1 (573–903), or MBP-LjNIN (551–878) recombinant proteins, consisting of an RWP-RK and a PB1 domain, were incubated with the FAM-labeled DNA probe (Supplemental Data Set 1). Blue, green, and red nucleotides indicate conserved motifs among the DNA fragments. Brackets and asterisks, respectively, indicate the position of shifted bands showing protein–DNA interaction and of free probes that did not interact with proteins. D, Transactivation of *LjCLE-RS2*$_{pro}$*:GUS* in *L. japonicus* mesophyll protoplasts transformed with respective constructs (n = 3 independent pools of protoplasts). *GFP*, *LjNLP4*, and *LjNLP1* used as effectors. Two types of *LjCLE-RS2*$_{pro}$*:GUS* reporter constructs were used, one with an intact *LjCLE-RS2* promoter and one with a modified *LjCLE-RS2* promoter in which the NRE/NBS (Figure 5C; Nishida et al., 2021) was specifically deleted (ΔNRE/NBS) (Supplemental Figure S6). Transformed protoplasts were incubated with 0 (−) or 10 mM (+) KNO_3. GUS activity was measured relative to 35S$_{pro}$*:LUC* activity. Transactivation data were normalized to the condition in which *GFP* was expressed in the absence of KNO_3. Error bars indicate SEM. Different letters indicate statistically significant differences ($P < 0.05$, one-way ANOVA followed by multiple comparisons).

together with the observation of abolished expression of *LjNRT2.1* in the *Ljnlp1* mutants (Figure 4A), the results from the transactivation assay indicate that LjNLP1 is necessary and sufficient to induce *LjNRT2.1* expression in response to nitrate.

To verify the protein–DNA interaction in more detail, we carried out an electrophoretic mobility shift assay (EMSA). The recombinant LjNLP1 and LjNIN proteins, consisting of an RWP-RK and a PB1 domain, bound to cis-elements of the *LjNRT2.1* promoter (Figure 5A). In contrast, the recombinant LjNLP4 protein with similar domains showed much weaker binding to the cis-elements (Figure 5A), which was consistent with the observation that LjNLP4 was not involved in the regulation of *LjNRT2.1* expression (Figure 4). As previously shown, LjNLP4 and LjNIN bound to cis-elements of *NITRITE REDUCTASE 1* (*LjNIR1*) and *LjCLE-RS2* promoters (Figure 5, B and C; Nishida et al., 2021). LjNLP1 also bound to the same regions (Figure 5, B and C). Transactivation assay showed that LjNLP1, as well as LjNLP4, could activate *LjCLE-RS2* expression through direct binding to the cis-element in a nitrate-dependent manner (Figure 5D; Supplemental Figure S6B).

LjNRT2.1, *LjNLP4*, and *LjNLP1* have overlapping expression patterns during nodulation

To determine spatial expression pattern of *LjNRT2.1* and its relevance to those of *LjNLP4* and *LjNLP1*, we conducted promoter-GUS reporter analysis. We first identified the functional promoter that could rescue the corresponding mutants to the same extent as constructs using the *LjUBQ* promoter, when used to express each gene (Supplemental Figure S7, A–C). The promoter fragments *LjNRT2.1*$_{pro}$ (3.2 kb), *LjNLP4*$_{pro}$ (2.3 kb) and *LjNLP1*$_{pro}$ (4.0 kb), harbored same regions as genomic fragments used in complementation assays (Supplemental Figure S2; Nishida et al., 2018, 2021). At initial developmental stages of nodulation, the

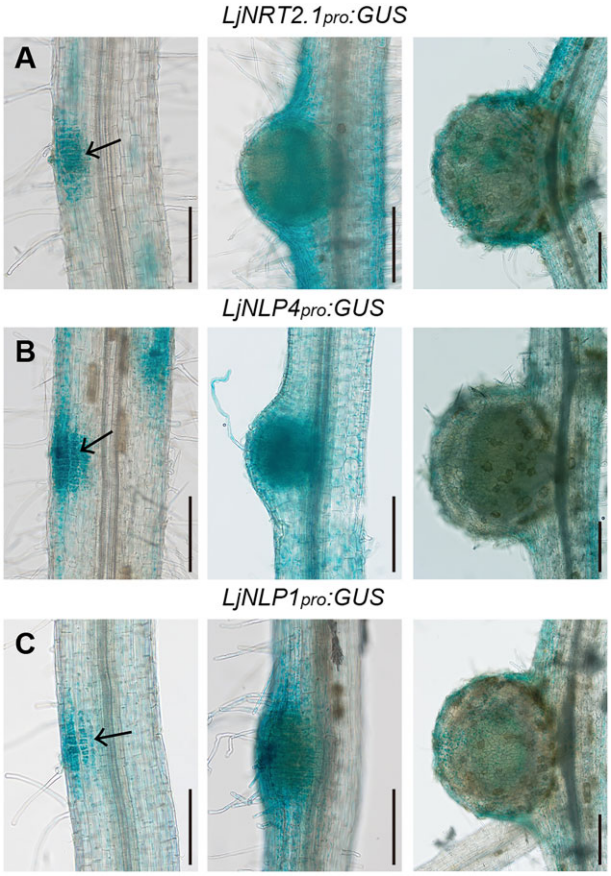

Figure 6 Spatial expression of *LjNRT2.1*, *LjNLP4*, and *LjNLP1* during nodulation. A–C, GUS activities in nodulating WT transgenic hairy roots transformed with the *LjNRT2.1*$_{pro}$*:GUS* (A), *LjNLP4*$_{pro}$*:GUS* (B), and *LjNLP1*$_{pro}$*:GUSplus* (C) constructs. Arrows indicate dividing cortical cells. Transgenic roots were identified by GFP fluorescence. Scale bars = 200 μm.

LjNRT2.1$_{pro}$*:GUS* construct showed that *LjNRT2.1* was expressed within dividing cortical cells, in an overlapping pattern with *LjNLP4* and *LjNLP1* (Figure 6). At later stages of nodulation, promoter-GUS constructs of each gene showed strong GUS activity in the outer regions of nodules, including epidermis. In addition to the expression in nodulation cell lineage, *LjNRT2.1* was expressed in the region of the root closer to the root base than the tip (Supplemental Figure S7D). Transverse sections of the region indicated that the *LjNRT2.1* was predominantly expressed in the epidermis (Supplemental Figure S7E). The epidermal *LjNRT2.1* expression might be insufficient to ensure the full LjNRT2.1 function, as the epidermis-specific expression of *LjNRT2.1* using the Epi promoter (Hayashi et al., 2014) failed to rescue the *Ljnrt2.1* phenotype (Supplemental Figure S7A).

Our data have shown that LjNLP1–LjNRT2.1 pathway has a role in nitrate-induced control of nodulation. We then asked if the expression of *LjNRT2.1* could compensate for LjNLP1 function. Constitutive *LjNRT2.1* expression from the *LjUBQ* promoter could not rescue the *Ljnlp1* mutation (Supplemental Figure S7C). Therefore, the expression of *LjNRT2.1* alone might be insufficient for nitrate-induced control of nodulation in the *Ljnlp1* mutants.

LjNRT2.1 function is linked to the nitrate-dependent regulation of LjNLP4 nuclear localization and control of symbiotic gene expression

One of the features of LjNLP4 is that its nuclear localization is regulated by nitrate (Nishida et al., 2018). Given the involvement of LjNRT2.1 and LjNLP1 in the nitrate-induced control of nodulation and the nitrate uptake/transport process, we verified that these proteins might be involved in regulating the subcellular localization of LjNLP4. In agreement with a previous study (Nishida et al., 2018), immunohistochemistry using an LjNLP4–myc fusion protein showed that LjNLP4 was localized within nuclei in response to nitrate in the WT (Figure 7A; Supplemental Figure S8A). In contrast, a strong signal for LjNLP4 was not evident in the nuclei of the *Ljnlp1* and the *Ljnrt2.1* mutants even in the presence of nitrate (Figure 7, B and C; Supplemental Figure S8A). RT-qPCR and immunoblot analysis indicated that the loss of nuclear LjNLP4 signals in the *Ljnlp1* and *Ljnrt2.1* mutants was not due to reduced *LjNLP4* expression nor LjNLP4 stability (Supplemental Figure S8, B and C). Therefore, our observations suggest that LjNLP1 and LjNRT2.1 act upstream of the nitrate-dependent LjNLP4 nuclear localization; LjNLP1-mediated activation of *LjNRT2.1* expression and subsequent nitrate transport may be required for LjNLP4 nuclear localization.

To further characterize the involvement of LjNRT2.1 in the nitrate-induced control of nodulation, we focused on the expression of symbiotic genes whose expression was affected by nitrate. Whereas nitrate upregulates the expression of *LjCLE-RS2*, nitrate downregulates the expression of *LjNF-YA*, *LjNF-YB*, and *LjEPR3* in an LjNLP4- and LjNLP1-dependent manner (Nishida et al., 2021). For RT-qPCR analysis, the WT and *Ljnrt2.1* plants were pretreated with nitrate for 24 h before rhizobial inoculation. Roots were collected at 3 days after inoculation (dai) with continuous nitrate treatment. Consequently, we found that the nitrate-induced level of *LjCLE-RS2* expression was lower in the *Ljnrt2.1* mutants than the WT (Figure 8A). In contrast, nitrate-repressed level of *LjNF-YA*, *LjNF-YB*, and *LjEPR3* was lower in the *Ljnrt2.1* mutants relative to the WT (Figure 8, B-D). These nitrate-induced/repressed expression patterns of the symbiotic genes in the *Ljnrt2.1* mutants resembled those in the *Ljnlp4* and the *Ljnlp1* mutants (Nishida et al., 2021). Furthermore, we found that the *LjNIN* expression was nitrate-repressible in WT and the nitrate-mediated reduction in *LjNIN* expression was abolished in the *Ljnrt2.1* mutants (Figure 8E).

LjNLP1 can substitute for LjNLP4 function

In addition to the phenotypic similarity of the mutants, our previous RNA-seq analysis indicated that LjNLP4 and LjNLP1 had mostly similar downstream genes (Nishida et al., 2021).

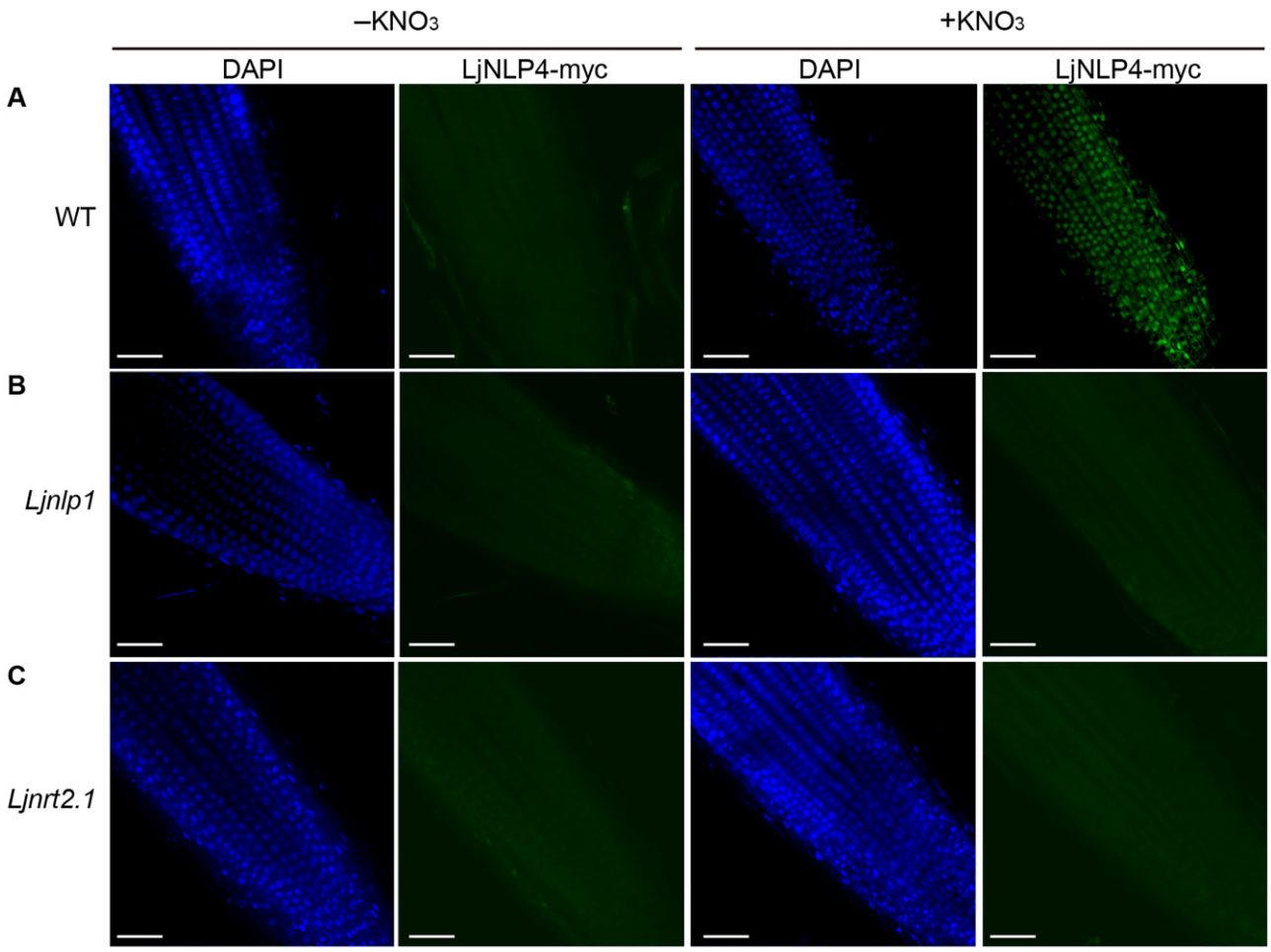

Figure 7 Subcellular localization of LjNLP4. A–C, Immunohistochemistry of the LjNLP4-myc protein in root apical cells of WT, *Ljnlp1*, and *Ljnrt2.1-1* mutants. A monoclonal anti-myc antibody and an antibody conjugated to Alexa Fluor 488 Plus (right: green signal) were used as the primary and secondary antibodies. Nuclei were visualized with DAPI (left: blue signal). Plants with transgenic hairy roots transformed with the *LjUBQ*$_{pro}$*:LjNLP4-myc* construct were grown on a nitrogen-free medium for 3 days and then supplied with 0 (−) or 10 mM KNO_3 (+) for 1 h. Representative images of at least five independent locations are shown for each condition. Scale bars = 50 μm.

Indeed, *LjCLE-RS2* was identified as a common direct target of LjNLP4 and LjNLP1 (Figure 5). These findings led us to postulate that the two NLPs might have overlapping functions. To examine the functional relationships of *LjNLP4* and *LjNLP1*, we expressed one gene in mutants of the other gene. The nodulation phenotype of the *Ljnlp4* mutants in the presence of nitrate was rescued by constitutive expression of *LjNLP1* (Figure 9A). In contrast, nodulation of the *Ljnlp1* mutants was unaffected by *LjNLP4* expression (Figure 9B). These results suggest that LjNLP1 can functionally substitute for LjNLP4.

LjNIN counteracts LjNLP1 function

A previous study showed that LjNIN inhibits the nitrate-inducible expression of *LjNRT2.1* and *LjNIR1* (Soyano et al., 2015). We sought to elucidate a more detailed mechanism underlying this LjNIN-mediated repression of nitrate-inducible gene expression. In transgenic hairy roots, *LjNIN* overexpression reduced the nitrate-induced levels of *LjNRT2.1* and *LjNIR1* (Figure 10, A–C), confirming a previous finding (Soyano et al., 2015). Since LjNLP1 has now been identified as a transcription factor that induces *LjNRT2.1* expression, and the NBS within the *LjNRT2.1*$_{pro}$ was required for the LjNLP1-dependent *LjNRT2.1* expression (Figures 4, B and 5, A), we reasoned that LjNIN might interfere with LjNLP1 function via protein–DNA interaction, thereby downregulating *LjNRT2.1* expression. To test this hypothesis, we first co-expressed *LjNLP1* and *LjNIN* in *L. japonicus* protoplasts and measured the expression of *LjNRT2.1*. The co-expression of LjNLP1 and LjNIN significantly reduced the relative expression level of *LjNRT2.1* compared to the case in which *LjNLP1* alone was expressed (Figure 10D). In addition, EMSA showed LjNLP1 and LjNIN bound competitively to the cis-element of *LjNRT2.1* promoter (Figure 10E).

Lastly, we investigated if rhizobial inoculation could influence nitrate uptake. To test this possibility, we measured the nitrate contents using inoculated and noninoculated WT plants grown without nitrate and then fed nitrate. The nitrate content in inoculated roots (7 dai) 24 h after nitrate treatment (10 mM) was lower than noninoculated roots of

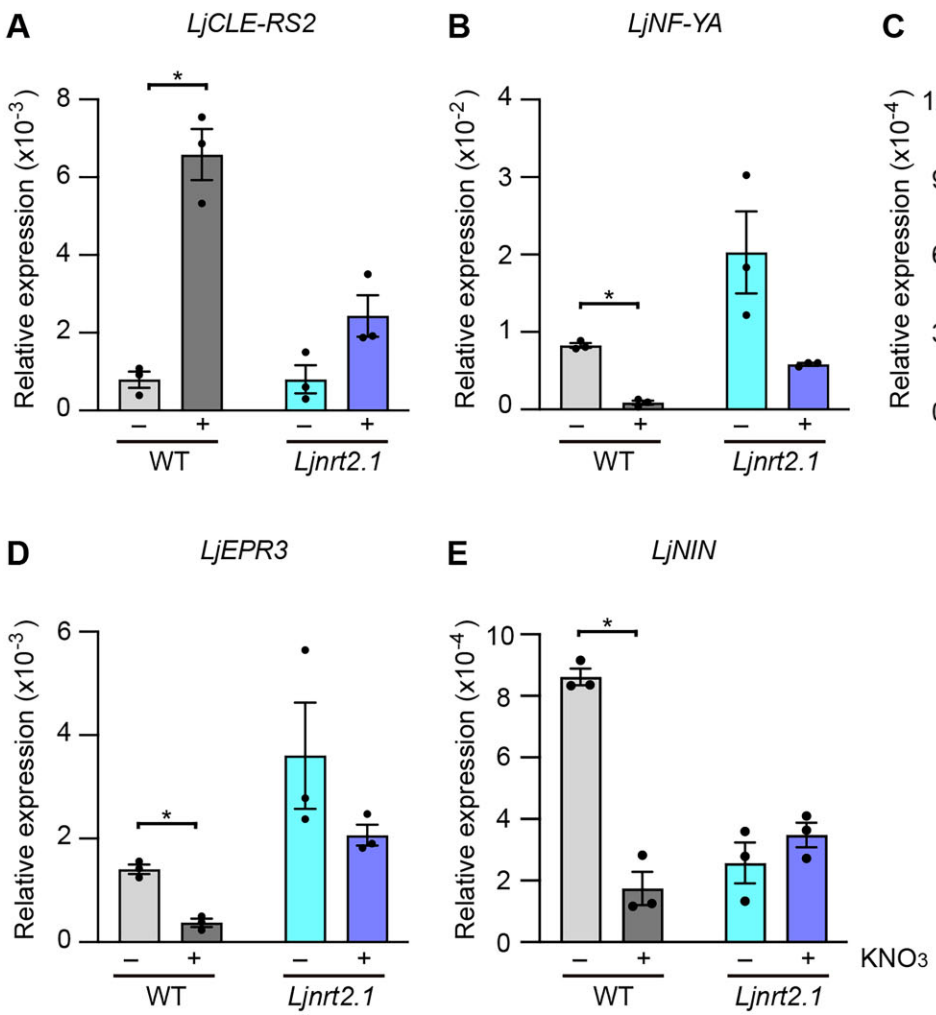

Figure 8 Symbiotic gene expression in the *Ljnrt2.1* mutants. A–E, RT-qPCR analysis of *LjCLE-RS2* (A), *LjNF-YA* (B), *LjNF-YB* (C), *LjEPR3* (D), and *LjNIN* (E) expression in the WT and *Ljnrt2.1-1* mutants. Plants were pretreated with 0 (–) or 10 mM KNO_3 (+) for 24 h before rhizobial inoculation. Roots at 3 dai with continuous treatment of 0 or 10 mM KNO_3 were collected (n = 3 independent pools of roots derived from three plants), and total RNA from the 3 dai roots was isolated for cDNA synthesis. The expression of *LjUBQ* was used as the reference. Error bars indicate SEM. *$P < 0.05$ by a two-sided Welch's t test.

the same age (Figure 10F). Of note, the rhizobia-dependent reduction in nitrate uptake was not observed in the *Ljnin* mutants (Figure 10F). Therefore, these data suggest that LjNIN has a role in modulating nitrate uptake by counteracting the LjNLP1 function that activates *LjNRT2.1* expression.

Discussion

The role of nitrate transporter genes in the nitrate-induced control of nodulation has been largely unknown. A recently identified gene, *MtNPF7.6*, is expressed in nodule transfer cells and mediates nitrate transport in nodules; *Mtnpf7.6* mutations affect the nitrate-induced control of nodulation (Wang et al., 2020). In our study, we showed that the *Ljnrt2.1* mutants maintained nodulation in high nitrate conditions. Although the MtNPF7.6 function appears to be restricted to nodules, LjNRT2.1 has a more general role in nitrate transport since it is involved in nitrate transport even in the absence of rhizobia.

In *L. japonicus*, LjNLP4 and LjNLP1 are known to have pivotal roles in transcriptional regulation in response to nitrate (Nishida et al., 2021); however, details about the genetic relationship of LjNLP4 and LjNLP1 have been incomplete. Here, we identified a critical functional difference between LjNLP4 and LjNLP1; LjNLP1 has an ability to induce *LjNRT2.1* expression perhaps because LjNLP1 can bind to a cis-element of the *LjNRT2.1* promoter more strongly than LjNLP4. *MtNRT2.1* expression was compromised by the mutation of *MtNLP1*, which is orthologous to *LjNLP1* (Lin et al., 2018). Therefore, the NLP1-NRT2.1 regulatory module may be conserved between *L. japonicus* and *M. truncatula*.

The nitrate uptake/transport process was attenuated not only by the *Ljnrt2.1* mutations but also by the *Ljnlp1* mutations. Nitrate-promoted shoot growth was more severely

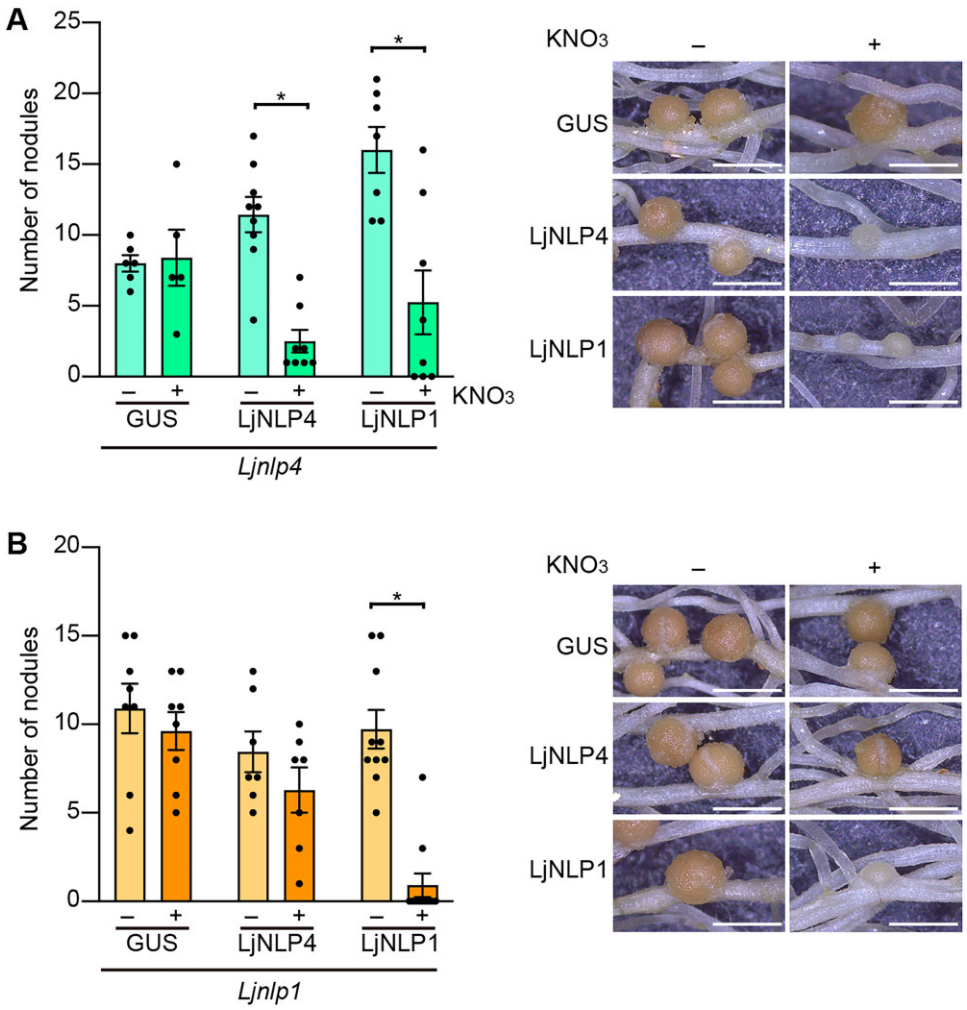

Figure 9 Reciprocal complementation assays of LjNLP4 and LjNLP1. A and B, Nodule number and nodulation phenotypes of transgenic hairy roots of the *Ljnlp4-1* (A) and *Ljnlp1* (B) mutants transformed with either the *LjUBQ*$_{pro}$*:GUS*, *LjUBQ*$_{pro}$*:LjNLP4*, or *LjUBQ*$_{pro}$*:LjNLP1* constructs in the presence of 0 (–) or 10 mM KNO_3 (+) at 21 dai (n = 6–11 plants). Transgenic roots were identified by GFP fluorescence. Error bars indicate SEM. *$P < 0.05$ by a two-sided Welch's t test. Scale bars = 1 mm.

affected in the *Ljnlp1* or the *Ljnrt2.1* mutants than the *Ljnlp4* mutants, an observation that may result from defects in nitrate uptake/transport. Phenotypic analysis using multiple mutants suggested that LjNRT2.1 acts in the same genetic pathway as LjNLP4 and LjNLP1 in the nitrate-induced control of nodulation. Furthermore, the nuclear localization of nitrate-dependent LjNLP4, a feature related to NLPs activity, was diminished by either the *Ljnlp1* or the *Ljnrt2.1* mutations.

Based on these observations and previous findings, we propose a signaling pathway model that acts in the nitrate-induced control of nodulation (Figure 11). In the model, LjNLP1 induces *LjNRT2.1* expression in the presence of exogenous nitrate. The activated LjNRT2.1 may enhance nitrate transport, which ultimately triggers LjNLP4 nuclear localization. Then, the expression of symbiotic genes is induced or repressed by LjNLP4 depending on the nature of their regulation; LjNLP4 acts synergistically to inhibit nodulation. Since the expression of *LjNRT2.1* was insufficient to rescue the *Ljnlp1* mutations, LjNLP1 likely has different downstream pathway from that includes LjNRT2.1 to control nodulation. Indeed, we demonstrated that LjNLP1 can directly induce *LjCLE-RS2* expression in response to nitrate. The NLP1-CLE regulatory module is also identified in *M. truncatula* (Luo et al., 2021). Considering LjNLP1's specific role in response to nitrate, LjNLP1 must be activated in some way by nitrate. Generally, there are two types of nitrate transporters in terms of gene expression pattern: whose expression is either constitutively expressed or is affected by nitrate (Cerezo et al., 2001; Krapp et al., 2014). An unknown constitutively expressed nitrate transporter independent of LjNRT2.1 may mediate the first step of nitrate uptake/transport to activate LjNLP1. Such a transporter may function similarly to AtNRT1.1, which is thought to act upstream of AtNLP6/7-mediated nitrate signaling (Liu et al., 2017). Our results also show that the expression of *LjNLP1* substituted for the *LjNLP4* function. Although the results need to be carefully interpreted, as a constitutive promoter (*LjUBQ*$_{pro}$) was used

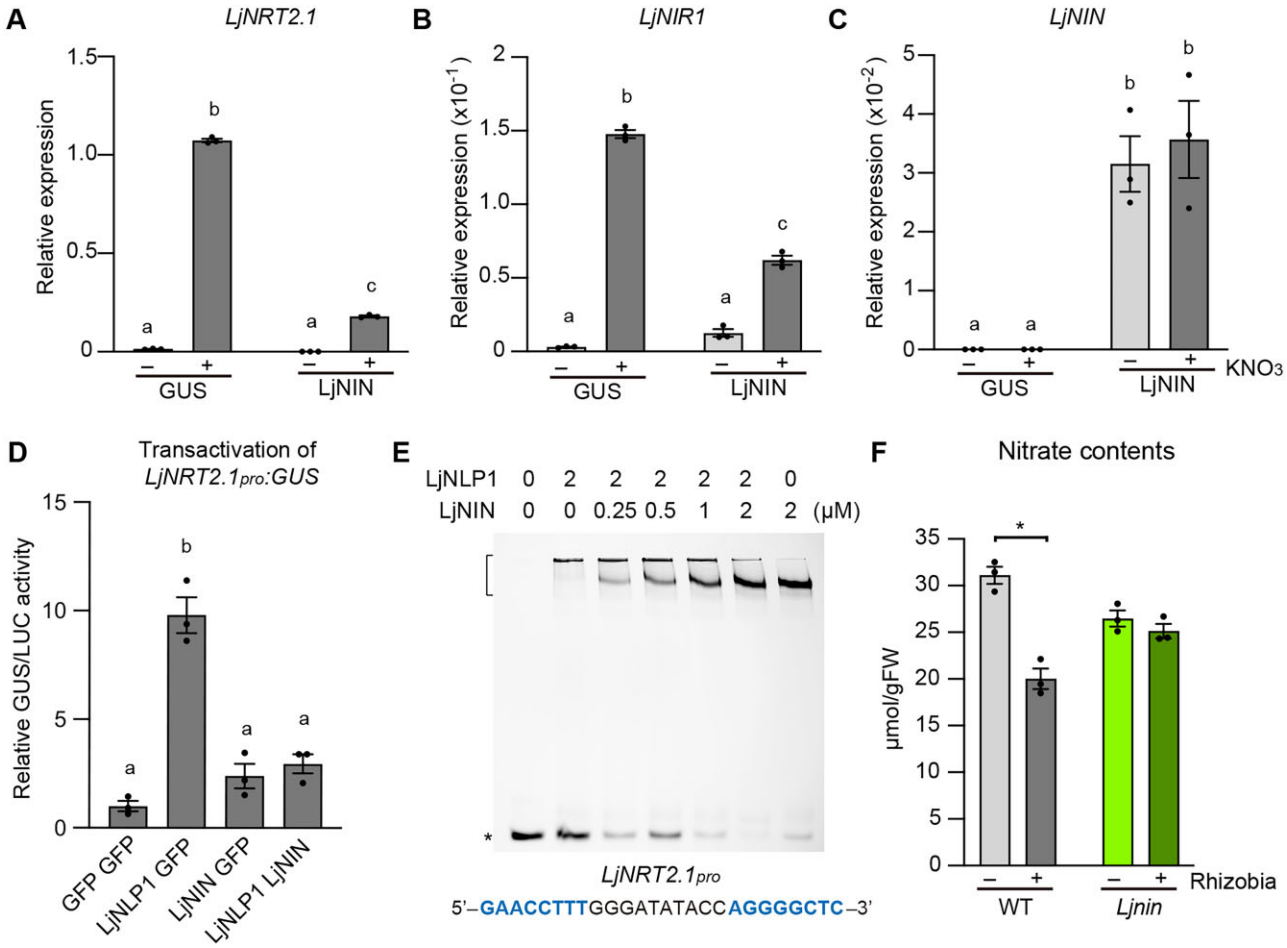

Figure 10 The regulation of *LjNRT2.1* expression by LjNIN. A–C, RT-qPCR analysis of *LjNRT2.1* (A), *LjNIR1* (B), and *LjNIN* (C) expression in WT transgenic hairy roots transformed with the *LjUBQ*$_{pro}$*:GUS* or *LjUBQ*$_{pro}$*:LjNIN* constructs. Each cDNA sample was prepared from total RNA derived from noninoculated roots pretreated with 0 (−) or 10 mM KNO_3 (+) for 24 h ($n = 3$ independent pools of roots derived from 10 plants). Transgenic roots were identified by GFP fluorescence. The expression of *LjUBQ* was used as the reference. Error bars indicate SEM. Different letters indicate statistically significant differences ($P < 0.05$, one-way ANOVA followed by multiple comparisons). D, Transactivation of *LjNRT2.1*$_{pro}$*:GUS* in *L. japonicus* mesophyll protoplasts transformed with three respective constructs ($n = 3$ independent pools of protoplasts). Transformed protoplasts were incubated with 10 mM KNO_3. GUS activity was measured relative to *35S*$_{pro}$*:LUC* activity. Transactivation data are normalized using the condition in which *GFP* is expressed. Different letters indicate statistically significant differences ($P < 0.05$, one-way ANOVA followed by multiple comparisons). E, EMSA showing LjNLP1 or LjNIN binding to the cis-elements on the *LjNRT2.1*$_{pro}$. MBP-LjNLP1 (573–903) or MBP-LjNIN (551–878) recombinant proteins, consisting of an RWP-RK and a PB1 domain, were incubated with the FAM-labeled DNA probe (Figure 5A; Supplemental Data Set 1). Concentration of the proteins is shown. Bracket and asterisk, respectively, indicate the position of shifted bands showing protein–DNA interaction and of free probes that did not interact with proteins. F, Nitrate contents in inoculated (7 dai) (+) and noninoculated (−) roots of the WT and *Ljnin-9* mutants ($n = 3$ independent pools of roots derived from four plants). The plants were first grown in each condition without KNO_3, incubated with 10 mM KNO_3 for 24 h, followed by measurement of the root nitrate contents. Error bars indicate SEM. *$P < 0.05$ by a two-sided Welch's *t* test.

in the assay, it is possible that LjNLP1 per se can regulate the expression of symbiotic genes in the same way as LjNLP4. Meanwhile, LjNLP4 was insufficient to replace LjNLP1's function, which is likely to reflect the fact that LjNLP4 could not induce *LjNRT2.1* expression. Elucidating the details of the functional overlap between LjNLP4 and LjNLP1 is a future challenge.

The temporal expression pattern of *LjNRT2.1* after nitrate treatment showed that nitrate-induced *LjNRT2.1* activation is transient, suggesting there is a feedback mechanism to control *LjNRT2.1* expression. Notably, *AtNRT2.1* expression is downregulated by nitrate assimilation products (Lejay et al., 1999). In the *Ljnlp4* mutants, the expression of *LjNIA* and *LjNIR1* genes was reduced (Nishida et al., 2018). Therefore, the higher levels of *LjNRT2.1* expression at later time points in the *Ljnlp4* mutants relative to the WT may be due to failed feedback regulation of *LjNRT2.1* by nitrate assimilation products. Although expression of the nitrate assimilation genes was also low in the *Ljnlp1* mutants (Nishida et al., 2021), *LjNRT2.1* expression was also compromised. Our

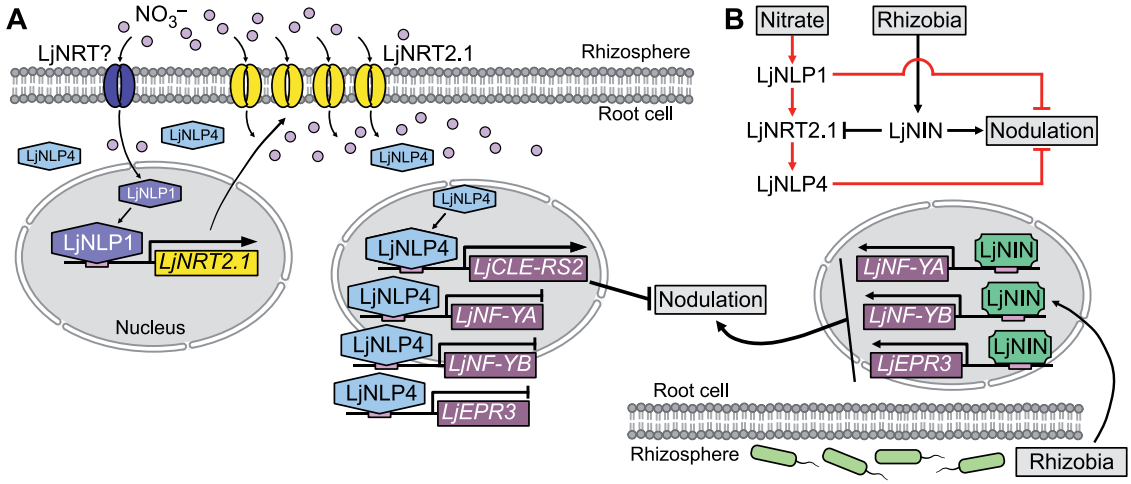

Figure 11 Model for the nitrate-induced control of nodulation in *L. japonicus*. A, A model of the LjNLP1-LjNRT2.1-LjNLP4 signaling pathway, which controls nodulation in response to nitrate. Nitrate taken up from the soil leads to activation of LjNLP1, thereby enabling LjNLP1 to induce the expression of *LjNRT2.1*. LjNRT2.1 then plays a role in enhancing nitrate uptake/transport. LjNLP4 nuclear localization is triggered by the enhanced influx of nitrate. LjNLP4 subsequently induces the expression of *LjCLE-RS2*, a negative regulator of nodulation. LjNLP4 also represses the expression of genes for positive regulators of nodulation, including *LjNF-YA*, *LjNF-YB*, and *LjEPR3*, by interfering with LjNIN's role in inducing these genes (Nishida et al., 2021). The resultant altered expression of these symbiotic genes acts synergistically to negatively regulate nodulation. B, A simplified model. In addition to the pathway including LjNRT2.1, LjNLP1 has a different downstream pathway to negatively regulate nodulation. Expression of *LjNIN*, a positive regulator of nodulation, is induced by rhizobial infection, and LjNIN has a role to block the LjNLP1-dependent expression of *LjNRT2.1*. Red indicates nitrate-related regulation.

interpretation of these results is that the defect in the induction of *LjNRT2.1* expression in the *Ljnlp1* mutants precedes that responsible for its feedback regulation by nitrate assimilation products.

How physiological processes in plants are regulated during root nodule symbiosis is poorly understood at the molecular level. Here, we provide a dataset that suggests that the nitrate uptake process can be modulated during nodulation. LjNIN, whose expression is induced specifically by rhizobial infection (Schauser et al., 1999; Suzaki et al., 2013), counteracts LjNLP1-dependent induction of *LjNRT2.1* expression (Figure 11). LjNIN and LjNLP1 have common cis-elements on the *LjNRT2.1* promoter. Importantly, the LjNIN–DNA interaction does not result in gene expression; instead, the interaction seems to block *LjNRT2.1* expression by LjNLP1. A previous study that supports our notion indicated that the expression of *LjNRT2.1* is downregulated by rhizobial inoculation (Criscuolo et al., 2012). Indeed, the negative regulation of *LjNRT2.1* by LjNIN is associated with a reduction in nitrate uptake. The physiological significance of this mechanism needs to be elucidated in the future; however, an attractive hypothesis is that this mechanism may be relevant to a switch in the plant's strategy concerning nitrogen acquisition. As nodule development progresses, legumes may switch from depending on nitrogen levels in the soil to symbiotic nitrogen fixation, thereby reducing soil nitrate uptake.

In Arabidopsis, the AtNRT2 family proteins are thought to play exclusive roles in HATS (Kiba et al., 2012; Krapp et al., 2014). AtNRT2.1 is responsible for 72% of HATS but is not involved in LATS (Wang et al., 1998; Filleur et al., 2001; Li et al., 2007). In *L. japonicus*, the effect of the *Ljnrt2.1* mutation was pronounced in the presence of high nitrate (10 mM). As far as we examined, WT and *Ljnrt2.1* mutants showed no obvious nodulation phenotypes at low nitrate concentrations. In addition, *LjNRT2.1* is required for nitrate transport irrelevant to the exogenous nitrate concentration. Hence, it is possible that the biochemical function of LjNRT2.1 differs from that of AtNRT2.1.

Many current research efforts to learn about plant adaptive strategies in nitrogen-deficient environments are primarily focused on Arabidopsis, a nonnodulating plant. Arabidopsis seems to have developed HATS to acquire low concentrations of soil nitrogen successfully (Kiba and Krapp, 2016; Oldroyd and Leyser, 2020). In contrast, it is enigmatic how nodulating plants such as legumes have adapted to nitrogen-deficient environments when they do not produce nodules. Given that coexistence with rhizobia is a prerequisite in nature, we propose that legumes have always depended on symbiotic nitrogen fixation and might not have needed to develop HATS. An observation potentially related to this hypothesis is that the number of *NRT2* family genes in legumes is lower than in Arabidopsis; there are three *NRT2* family genes in *L. japonicus* and *M. truncatula*, five members in soybean, and seven *NRT2* family genes in Arabidopsis (Valkov et al., 2020). A comparative functional analysis of *NRT2* family genes in the future may provide clues for elucidating the conserved and diverse roles of nitrate transport systems in nodulating and nonnodulating plants.

Materials and methods

Plant materials and growth conditions

The Miyakojima MG-20 ecotype of *L. japonicus* was used as the WT plant (Kawaguchi, 2000). The *nrsym3* and *nrsym4* mutants were isolated in a previous screening for EMS

mutants involved in the nitrate response during nodulation (Nishida et al., 2018). The *Ljnrt2.1-1* mutants were backcrossed with WT once and descendent *Ljnrt2.1-1* mutants were used for all analyses in this study. A description of *Ljnlp4-1*, *Ljnlp1*, and *Ljnin-9* plants was published previously (Yoro et al., 2014; Nishida et al., 2018, 2021). Plants were grown with or without *Mesorhizobium loti* MAFF 303099 in autoclaved vermiculite or on 1% agar plates with Broughton and Dilworth (B&D; Broughton and Dilworth, 1971) solution under a 16-h light/8-h dark cycle at 24°C.

Genome-resequencing of the *nrsym3* and *nrsym4* mutants

The *nrsym3* and *nrsym4* mutants were crossed with MG-52, and F2 progeny displaying nitrate-tolerant phenotype were screened. Genomic DNA was extracted from pools of leaves derived from 20 plants using a DNeasy Plant Mini Kit (Qiagen, Hilden, Germany). Libraries were constructed using a TruSeq DNA Sample Prep Kit (Illumina, San Diego, CA, USA) and sequenced using a NextSeq 500 (Illumina) instrument with an 86-bp single-end sequencing protocol. Reads were mapped against the *L. japonicus* genome version 3.0 (http://www.kazusa.or.jp/lotus/) by Bowtie-0.12.9 (Langmead et al., 2009). Single-nucleotide polymorphism candidates were identified using the Mitsucal program (Suzuki et al., 2018).

Phylogenetic analysis

Phylogenetic analysis was conducted in MEGA X. The phylogenetic tree was built using the Neighbor-Joining method. The optimal tree with the sum of branch length = 2.47369594 was shown. The percentage of replicate trees in which the associated taxa clustered together in the bootstrap test (1,000 replicates) are shown next to the branches. The tree is drawn to scale, with branch lengths in the same units as those of the evolutionary distances used to infer the phylogenetic tree. The evolutionary distances were computed using the Poisson correction method and were in the units of the number of amino acid substitutions per site. All positions containing gaps and missing data were eliminated (complete deletion option). Sequence alignment and machine-readable tree files are provided as Supplemental Files S1 and S2, respectively.

Constructs

The primers used for PCR are shown in Supplemental Data Set 1. For the complementation analysis of the *nrsym3* mutants, a 6.4-kb genomic DNA fragment including the *LjNRT2.1* candidate gene was amplified by PCR from WT genomic DNA. This fragment, including a 3.2-kb sequence directly upstream of the initiation codon, was cloned into pCAMBIA1300-GFP (Suzaki et al., 2019). For promoter-GUS analysis using *L. japonicus* hairy roots, a 3.2-kb fragment of the *LjNRT2.1* promoter region was amplified by PCR from WT genomic DNA and cloned upstream of the *GUS* gene in the pCAMBIA1300-GUS-GFP-LjLTI6b vector (Nishida et al., 2016). For making $LjNLP1_{pro}$:*GUSplus*:$LjNLP1_{ter}$, $LjNLP1_{pro}$:*LjNLP1*:$LjNLP1_{ter}$, and $LjNLP4_{pro}$:*LjNLP4-myc* constructs, each DNA fragment was amplified by PCR from WT genomic DNA, cDNA, or original vectors (Nishida et al., 2018; Suzaki et al., 2019) and inserted in pCAMBIA1300-GFP by the In-Fusion (Clontech, Mountain View, CA, USA) reaction. $LjNLP4_{pro}$:*GUS* construct was previously created (Nishida et al., 2018). For epidermis-specific expression, first DNA fragments of $Epi308_{pro}$ and NOS_{ter} were amplified from an original vector (Hayashi et al., 2014) and inserted in pCAMBIA1300-GFP by the In-Fusion reaction. Then, the *LjNRT2.1* CDS was inserted downstream of $Epi308_{pro}$ by the In-Fusion reaction. To make the constructs for recombinant protein expression in *Escherichia coli*, a gene encoding maltose-binding protein (MBP) and a portion of *LjNLP1* (573–903) was fused in the expression vector pMAL-c2X (New England Biolabs, Ipswich, MA, USA) by the In-Fusion reaction. MBP-LjNLP4 (564–976) and MBP-LjNIN (551–878) were previously created (Nishida et al., 2021). For the transactivation assay using protoplasts, *LjNLP1* CDS was amplified by PCR from template cDNA prepared from WT roots and inserted downstream of $LjUBQ_{pro}$ in the vector with pUC19 backbone (Nishida et al., 2021) by the In-Fusion reaction. A 3.2-kb fragment of the *LjNRT2.1* promoter region was amplified by PCR from WT genomic DNA and inserted upstream of *GUS-*$RBCS_{ter}$ cassette in the vector with pUC19 backbone (Nishida et al., 2021) by the In-Fusion reaction. To make the *LjNRT2.1*$(\Delta NBS)_{pro}$:*GUS* construct, the upstream and downstream regions across the LjNIN-binding site on the *LjNRT2.1* promoter were, respectively, amplified by PCR and ligated using PstI site and inserted upstream of *GUS-*$RBCS_{ter}$ cassette in the vector with pUC19 backbone (Nishida et al., 2021) by the In-Fusion reaction. The DNA fragments of a part of $LjCLE\text{-}RS2_{pro}$ fused with 35S minimal promoter with or without LjNLP4/LjNIN-binding sequence (NRE/NBS) were artificially synthesized based on previous finding (Soyano et al., 2014). They were amplified by PCR and inserted upstream of *GUS-*$RBCS_{ter}$ cassette in the vector with pUC19 backbone (Nishida et al., 2021) by the In-Fusion reaction. Other constructs, $LjUBQ_{pro}$:*GFP*, $LjUBQ_{pro}$:*LjNLP4*, $LjUBQ_{pro}$:*LjNIN*, and $35S_{pro}$:*LUC*, were previously created (Nishida et al., 2021). A previously created $LjUBQ_{pro}$:*LjNLP4-myc* construct (Nishida et al., 2018) was used for immunohistochemistry. For *LjNRT2.1*, *LjNLP4*, or *LjNLP1* overexpression in *L. japonicus* hairy roots, CDS of each gene was amplified by PCR from template cDNA prepared from WT roots and was cloned into the pENTR/D-TOPO vector (Invitrogen, Waltham, MA, USA). The insert was transferred into pUB-GW-GFP (Maekawa et al., 2008) by the LR recombination reaction. The $LjUBQ_{pro}$:*GUS* or $LjUBQ_{pro}$:*LjNIN* constructs for hairy roots transformation were described previously (Suzaki et al., 2012; Nishida et al., 2018).

Hairy root transformation of *L. japonicus*

Respective constructs were introduced into *A. rhizogenes* AR1193 strain. Hairy root transformation of *L. japonicus* was conducted based on the method (Okamoto et al., 2013).

Measurement of nitrate uptake and contents

For the analysis using an ^{15}N stable isotope, samples were prepared based on the method described previously (Tabata et al., 2014). In inoculated conditions, plants were grown with 0.2 or 5mM KNO_3 in the presence of rhizobia for 12 days, and plants were then treated with 0.2 or 5mM $K^{15}NO_3$ for 24 h. In noninoculated conditions, 12-day-old noninoculated seedlings grown on B&D medium without KNO_3 were transferred to new B&D medium with 0.2 or 10mM KNO_3 for 12 h. Then, they were washed by 0.1mM $CaSO_4$ for 1 min and transferred to B&D medium with 0.2 or 10mM $K^{15}NO_3$ for 5 min. At the end of the ^{15}N labeling, roots were washed for 1 min in 0.1mM $CaSO_4$ and were separated from shoots. Each sample was dried for 2 days at 75°C and analyzed for total N and ^{15}N contents by elemental analysis–isotope ratio mass spectrometry (Flash 2000-DELTA plus Advantage ConFlo III System; Thermo Fisher Scientific, Waltham, MA, USA).

Nitrate contents were measured based on the method previously described (Hachiya and Okamoto, 2017). Seedlings grown under each experimental condition were treated with 10mM KNO_3. Then, they were washed by sterilized water and frozen by liquid nitrogen. Each sample was crushed using a TissueLyser II (Qiagen), and 10 μL of sterilized water at 80°C was added per 1 mg of sample weight, and vortexing was performed every 5 min for 20 min at 100°C. The sample was then chilled on ice and spun down. The supernatant was stored as extraction solution at −80°C. About 20 μL of 0.05% salicylic acid in sulfuric acid or sulfuric acid was added to 5 μL of extraction solution in a tube, which was vortexed, spun down, and left at room temperature for 20 min. Then, 500 μL of 8% NaOH in sterilized water was added and the mixture was vortexed until it became clear. Nitrate content in the solution was determined by absorbance at 410 nm using a Multiskan GO (Thermo Fisher Scientific) or a Synergy LX (Biotek, Winooski, VT, USA).

EMSA

Recombinant proteins were prepared based on the method previously described (Nishida et al., 2021). For preparing the probes, DNA fragments (Supplemental Data Set 1) were labeled with carboxyfluorescein (FAM). The labeled DNA fragments were purified on the Superdex 200 10/300 GL column (GE Healthcare, Chicago, IL, USA). The purified DNA fragments (0.25 μM) and poly (dI-dC) (50 ng/μL) were mixed with the purified proteins in buffer D (10mM Tris–HCl pH 7.5, 100mM KCl, 100mM NaCl, 1mM DTT, 2.5% glycerol, and 5mM $MgCl_2$), and incubated at 25°C for 30 min. The mixtures were loaded on a 10% polyacrylamide gel, and fluorescence was detected using LuminoGraph III WSE-6300 (ATTO, Tokyo, Japan).

Gene expression analysis

The primers used for PCR are shown in Supplemental Data Set 1. Total RNA was isolated from whole roots using the PureLink Plant RNA Reagent (Invitrogen) or the Plant Total RNA Mini Kit (Favorgen Biotech, Ping-Tung, Taiwan). First-strand cDNA was prepared using the ReverTra Ace qPCR RT Master Mix with gDNA Remover (Toyobo, Osaka, Japan). RT-qPCR was performed using a 7900HT Real-Time PCR system (Applied Biosystems Waltham, MA, USA) with a THUNDERBIRD SYBR qPCR Mix (Toyobo) following the manufacturer's instructions.

Immunohistochemistry

Immunohistochemistry was conducted based on the method (Nishida et al., 2018). A monoclonal anti-myc antibody and an antibody conjugated to Alexa Fluor 488 Plus anti-mouse IgG-Alexa Fluor Plus 488 (Invitrogen) were used for detecting the signal derived from LjNLP4-myc. Before observing the signal, the roots were stained with 5μg mL^{-1} 4′, 6-diamidino-2-phenylindole (DAPI; Dojindo, Kumamoto, Japan) for 15 min. Fluorescent images were obtained using an LSM700 confocal laser-scanning microscope (Carl Zeiss, Oberkochen, Germany) equipped with ZEN software (Carl Zeiss). The obtained images were analyzed using ImageJ; first, the threshold of the green signals derived from LjNLP4-myc was set equally among the images, and then the ratio of the number of the nuclei with green signals was quantified against the number of the total, namely DAPI-stained, nuclei in every image.

Transactivation using *L. japonicus* protoplasts

The isolation of *L. japonicus* mesophyll protoplasts and the transactivation assay were conducted based on the method (Nishida et al., 2021). To exclude the effect of endogenous nitrate on gene expression, plants were grown without nitrate but with 10mM NH_4Cl for 16 days. Fluorescence and luminescence were measured using a Synergy LX (Biotek). For transformation of protoplasts, equal amount of DNA (10 μg each) of effector, reporter and internal control plasmids were used. $35S_{pro}$:*LUC* was used as the internal control plasmid.

Immunoblot analysis

The plants with transgenic hairy roots were treated with 10mM KNO_3 for 1 h, and their roots (150 mg), which were derived from five plants, were ground by bead beating after freezing with liquid nitrogen. Lysis buffer (50mM Tris–HCl, pH 8.0, 120mM NaCl, 0.2mM sodium orthovanadate, 100mM NaF, 10% glycerol, 0.2% Triton X-100, 5mM DTT, 5mM EDTA, 1mM PMSF, and 1× protein inhibitor cocktail [Nacalai Tesque, Kyoto, Japan]) were added. The ground roots and buffer were thoroughly mixed by bead beating, and then sonicated on ice. The suspension was centrifuged at 20,000 *g* for 20 min at 4°C. The supernatant was collected and subjected to sodium dodecyl sulfate polyacrylamide gel electrophoresis (SDS-PAGE) using 4%–15% Mini-PROTEAN TG Precast Protein Gels (Bio-Rad, Hercules, CA, USA). The separated proteins were electrically transferred onto a PVDF membrane (Amersham Hybond P PVDF; GE Healthcare). A primary antibody against c-Myc (Santa Crux Biotechnology, Dallas, TX, USA; catalog no. c-789) diluted in blocking buffer (1% bovine standard albumin and 1% polyvinylpyrrolidone

in TBST buffer [Tris-buffered saline, 0.1% Tween-20]) was applied to the membrane for overnight incubation at 4°C. After extensive washing, a Horseradish Peroxidase (HRP)-conjugated secondary antibody (Rockland; catalog no. 18-8816-31) diluted in the same blocking buffer was applied for 1 h at room temperature. Immobilon Forte Western HRP substrate (Merck, Kenilworth, NJ, USA) chemiluminescence reagent was used to detect antibody binding. Signals were detected using LuminoGraph III WSE-6300 (ATTO). For antibody stripping, the membrane was incubated in stripping buffer (6.4mM Tris–HCl, pH 6.8, 2% SDS, and 10mM DTT) for 45 min at 50°C. After being washed by the TBST buffer, the membrane was incubated with a primary antibody against GFP (Invitrogen; catalog no. A11122) diluted in blocking buffer. The antibody binding was detected in the same way as above.

Statistical analysis

Statistical analysis was performed using GraphPad Prism version 9 (GraphPad Software, San Diego, CA, USA). Normality was checked using the Shapiro-Wilk test and $P > 0.05$ was considered as normal distribution. The F-test was used to test if the variances of two populations were equal or not. Appropriate methods were chosen according to the nature of the data. The criterion of $P < 0.05$ means statistically significant difference in this study. The results of the statistical analyses are shown in Supplemental Data Set 2.

Accession number

Data from the short reads from genome-resequencing of *nrsym3* and *nrsym4* were deposited in the DNA Data Bank of Japan Sequence Read Archive under the accession number DRA011845.

Supplemental data

The following materials are available in the online version of this article.

Supplemental Figure S1. Allelism test of the *nrsym3* and the *nrsym4* mutants (Supports Figure 1).

Supplemental Figure S2. Complementation of the *nrsym3* phenotypes (Supports Figure 1).

Supplemental Figure S3. Comparison of LjNRT2.1 and LjNRT2.2 (Supports Figure 1).

Supplemental Figure S4. Nitrate effects on nodulation of multiple combinations of mutants among *Ljnlp4*, *Ljnlp1*, and *Ljnrt2.1* (Supports Figure 2).

Supplemental Figure S5. Effects of the *Ljnrt2.1* mutations on nitrate uptake and gene expression (Supports Figure 3).

Supplemental Figure S6. A schematic diagram of the promoter-GUS constructs used in transactivation assay (Supports Figures 4 and 5).

Supplemental Figure S7. Complementation of the *Ljnrt2.1*, *Ljnlp4*, and *Ljnlp1* phenotypes and *LjNRT2.1*$_{pro}$*:GUS* (Supports Figure 6).

Supplemental Figure S8. The ratio of LjNLP4-accumulating nuclei in immunohistochemistry (Supports Figure 7).

Supplemental Data Set 1. Primers used in this study.

Supplemental Data Set 2. Statistical analysis data.

Supplemental File S1. Sequence alignment of NRT2s in fasta format.

Supplemental File S2. Phylogenetic tree in newick format.

Acknowledgments

We thank Yoshikatsu Matsubayashi and Takatoshi Kiba for valuable suggestions; Takushi Hachiya and Kazuko Ito for technical support; Haruko Imaizumi-Anraku for providing Epi$_{pro}$ vector.

Funding

This work was supported by Ministry of Education, Culture, Sports, Science and Technology (MEXT) KAKENHI (JP19H03239 and JP20H05908), by Japan Science Technology Agency (JST) Exploratory Research for Advanced Technology (ERATO) (JPMJER1502).

Conflict of interest statement. The authors declare no conflict of interests.

References

Broughton WJ, Dilworth MJ (1971) Control of leghaemoglobin synthesis in snake beans. Biochem J **125:** 1075–1080

Carroll BJ, Mathews A (1990) Nitrate inhibition of nodulation in legumes. *In* PM Gresshof, ed, The Molecular Biology of Symbiotic Nitrogen Fixation, CRC Press, Boca Raton, FL, pp 159–180

Carroll BJ, McNeil DL, Gresshoff PM (1985) A supernodulation and nitrate-tolerant symbiotic (*nts*) soybean mutant. Plant Physiol **78:** 34–40

Cerezo M, Tillard P, Filleur S, Munos SP, Daniel-Vedele FO, Gojon A (2001) Major alterations of the regulation of root NO_3^- uptake are associated with the mutation of *Nrt2.1* and *Nrt2.2* genes in *Arabidopsis*. Plant Physiol **127:** 262–271

Criscuolo G, Valkov VT, Parlati A, Alves LM, Chiurazzi M (2012) Molecular characterization of the *Lotus japonicus NRT1(PTR)* and *NRT2* families. Plant Cell Environ **35:** 1567–1581

Filleur S, Dorbe MF, Cerezo M, Orsel M, Granier F, Gojon A, Daniel-Vedele F (2001) An *Arabidopsis* T-DNA mutant affected in *Nrt2* genes is impaired in nitrate uptake. FEBS Lett **489:** 220–224

Hachiya T, Okamoto Y (2017) Simple spectroscopic determination of nitrate, nitrite, and ammonium in *Arabidopsis thaliana*. Bio-protocol **7:** e2280

Hayashi T, Shimoda Y, Sato S, Tabata S, Imaizumi-Anraku H, Hayashi M (2014) Rhizobial infection does not require cortical expression of upstream common symbiosis genes responsible for the induction of Ca^{2+} spiking. Plant J **77:** 146–159

Ho CH, Lin SH, Hu HC, Tsay YF (2009) CHL1 functions as a nitrate sensor in plants. Cell **138:** 1184–1194

Kawaguchi M (2000) *Lotus japonicus* `Miyakojima' MG-20: an early-flowering accession suitable for indoor handling. J Plant Res **113:** 507–509

Kawaharada Y, Kelly S, Nielsen MW, Hjuler CT, Gysel K, Muszynski A, Carlson RW, Thygesen MB, Sandal N, Asmussen MH, et al. (2015) Receptor-mediated exopolysaccharide perception controls bacterial infection. Nature **523:** 308–312

Kawaharada Y, Nielsen MW, Kelly S, James EK, Andersen KR, Rasmussen SR, Füchtbauer W, Madsen LH, Heckmann AB, Radutoiu S, et al. (2017) Differential regulation of the *Epr3* receptor coordinates membrane-restricted rhizobial colonization of root nodule primordia. Nat Commun **8:** 14534

Kiba T, Feria-Bourrellier AB, Lafouge F, Lezhneva L, Boutet-Mercey S, Orsel M, Bréhaut V, Miller A, Daniel-Vedele F, Sakakibara H, et al. (2012) The *Arabidopsis* nitrate transporter NRT2.4 plays a double role in roots and shoots of nitrogen-starved plants. Plant Cell **24:** 245–258

Kiba T, Krapp A (2016) Plant nitrogen acquisition under low availability: regulation of uptake and root architecture. Plant Cell Physiol **57:** 707–714

Krapp A, David LC, Chardin C, Girin T, Marmagne A, Leprince AS, Chaillou S, Ferrario-Méry S, Meyer C, Daniel-Vedele F (2014) Nitrate transport and signalling in *Arabidopsis*. J Exp Bot **65:** 789–798

Krusell L, Madsen LH, Sato S, Aubert G, Genua A, Szczyglowski K, Duc G, Kaneko T, Tabata S, de Bruijn F, et al. (2002) Shoot control of root development and nodulation is mediated by a receptor-like kinase. Nature **420:** 422–426

Laffont C, Ivanovici A, Gautrat P, Brault M, Djordjevic MA, Frugier F (2020) The NIN transcription factor coordinates CEP and CLE signaling peptides that regulate nodulation antagonistically. Nat Commun **11:** 3167

Langmead B, Trapnell C, Pop M, Salzberg SL (2009) Ultrafast and memory-efficient alignment of short DNA sequences to the human genome. Genome Biol **10:** R25

Lejay L, Tillard P, Lepetit M, Olive FD, Filleur S, Daniel-Vedele F, Gojon A (1999) Molecular and functional regulation of two NO_3 uptake systems by N- and C-status of *Arabidopsis* plants. Plant J **18:** 509–519

Li W, Wang Y, Okamoto M, Crawford NM, Siddiqi MY, Glass ADM (2007) Dissection of the *AtNRT2.1*:*AtNRT2.2* inducible high-affinity nitrate transporter gene cluster. Plant Physiol **143:** 425–433

Li X, Zheng Z, Kong X, Xu J, Qiu L, Sun J, Reid D, Jin H, Andersen SU, Oldroyd GED, Stougaard J, Downie JA, et al. (2019) Atypical receptor kinase RINRK1 required for rhizobial infection but not nodule development in *Lotus japonicus*. Plant Physiol **181:** 804–816

Lin JS, Li X, Luo Z, Mysore KS, Wen J, Xie F (2018) NIN interacts with NLPs to mediate nitrate inhibition of nodulation in *Medicago truncatula*. Nat Plants **4:** 942–952

Liu KH, Niu Y, Konishi M, Wu Y, Du H, Sun Chung H, Li L, Boudsocq M, McCormack M, Maekawa S, Ishida T, Zhang C, et al. (2017) Discovery of nitrate–CPK–NLP signalling in central nutrient–growth networks. Nature **545:** 311–316

Luo Z, Lin JS, Zhu Y, Fu M, Li X, Xie F (2021) NLP1 reciprocally regulates nitrate inhibition of nodulation through SUNN-CRA2 signaling in *Medicago truncatula*. Plant Commun **2:** 100183

Maekawa T, Kusakabe M, Shimoda Y, Sato S, Tabata S, Murooka Y, Hayashi M (2008) Polyubiquitin promoter-based binary vectors for overexpression and gene silencing in *Lotus japonicus*. Mol Plant-Microbe Interact **21:** 375–382

Marchive C, Roudier F, Castaings L, Bréhaut V, Blondet E, Colot V, Meyer C, Krapp A (2013) Nuclear retention of the transcription factor NLP7 orchestrates the early response to nitrate in plants. Nat Commun **4:** 1713

Mens C, Hastwell AH, Su H, Gresshoff PM, Mathesius U, Ferguson BJ (2021) Characterisation of *Medicago truncatula CLE34* and *CLE35* in nitrate and rhizobia regulation of nodulation. New Phytol **229:** 2525–2534

Moreau C, Gautrat P, Frugier F (2021) Nitrate-induced CLE35 signaling peptides inhibit nodulation through the SUNN receptor and miR2111 repression. Plant Physiol **185:** 1216–1228

Murray JD (2011) Invasion by invitation: rhizobial infection in legumes. Mol Plant-Microbe Interact **24:** 631–639

Nishida H, Handa Y, Tanaka S, Suzaki T, Kawaguchi M (2016) Expression of the *CLE-RS3* gene suppresses root nodulation in *Lotus japonicus*. J Plant Res **129:** 909–919

Nishida H, Ito M, Miura K, Kawaguchi M, Suzaki T (2020) Autoregulation of nodulation pathway is dispensable for nitrate-induced control of rhizobial infection. Plant Signal Behav **15:** 1733814

Nishida H, Nosaki S, Suzuki T, Ito M, Miyakawa T, Nomoto M, Tada Y, Miura K, Tanokura M, Kawaguchi M, et al. (2021) Different DNA-binding specificities of NLP and NIN transcription factors underlie nitrate-induced control of root nodulation. Plant Cell **33:** 2340–2359

Nishida H, Suzaki T (2018a) Two negative regulatory systems of root nodule symbiosis: how are symbiotic benefits and costs balanced? Plant Cell Physiol **59:** 1733–1738

Nishida H, Suzaki T (2018b) Nitrate-mediated control of root nodule symbiosis. Curr Opin Plant Biol **44:** 129–136

Nishida H, Tanaka S, Handa Y, Ito M, Sakamoto Y, Matsunaga S, Betsuyaku S, Miura K, Soyano T, Kawaguchi M, et al. (2018) A NIN-LIKE PROTEIN mediates nitrate-induced control of root nodule symbiosis in *Lotus japonicus*. Nat Commun **9:** 499

Nishimura R, Hayashi M, Wu GJ, Kouchi H, Imaizumi-Anraku H, Murakami Y, Kawasaki S, Akao S, Ohmori M, Nagasawa M, et al. (2002) HAR1 mediates systemic regulation of symbiotic organ development. Nature **420:** 426–429

Okamoto S, Ohnishi E, Sato S, Takahashi H, Nakazono M, Tabata S, Kawaguchi M (2009) Nod factor/nitrate-induced *CLE* genes that drive HAR1-mediated systemic regulation of nodulation. Plant Cell Physiol **50:** 67–77

Okamoto S, Yoro E, Suzaki T, Kawaguchi M (2013) Hairy root transformation in *Lotus japonicus*. Bio-protocol **3:** e795

Oldroyd GE, Murray JD, Poole PS, Downie JA (2011) The rules of engagement in the legume-rhizobial symbiosis. Annu Rev Genet **45:** 119–144

Oldroyd GED, Leyser O (2020) A plant's diet, surviving in a variable nutrient environment. Science **368:** eaba0196

Pellizzaro A, Alibert B, Planchet E, Limami AM, Morère-Le Paven MC (2017) Nitrate transporters: an overview in legumes. Planta **246:** 585–595

Roy S, Liu W, Nandety RS, Crook A, Mysore KS, Pislariu CI, Frugoli J, Dickstein R, Udvardi MK (2020) Celebrating 20 years of genetic discoveries in legume nodulation and symbiotic nitrogen fixation. Plant Cell **32**: 15–41

Schauser L, Roussis A, Stiller J, Stougaard J (1999) A plant regulator controlling development of symbiotic root nodules. Nature **402:** 191–195

Schauser L, Wieloch W, Stougaard J (2005) Evolution of NIN-like proteins in *Arabidopsis*, rice, and *Lotus japonicus*. J Mol Evol **60:** 229–237

Schnabel E, Journet EP, de Carvalho-Niebel F, Duc G, Frugoli J (2005) The *Medicago truncatula SUNN* gene encodes a CLV1-like leucine-rich repeat receptor kinase that regulates nodule number and root length. Plant Mol Biol **58:** 809–822

Searle IR, Men AE, Laniya TS, Buzas DM, Iturbe-Ormaetxe I, Carroll BJ, Gresshoff PM (2003) Long-distance signaling in nodulation directed by a CLAVATA1-like receptor kinase. Science **299:** 109–112

Shrestha A, Zhong S, Therrien J, Huebert T, Sato S, Mun T, Andersen SU, Stougaard J, Lepage A, Niebel A, et al. (2021) *Lotus japonicus Nuclear Factor YA1*, a nodule emergence stage-specific regulator of auxin signalling. New Phytol **229:** 1535–1552

Soyano T, Hirakawa H, Sato S, Hayashi M, Kawaguchi M (2014) NODULE INCEPTION creates a long-distance negative feedback loop involved in homeostatic regulation of nodule organ production. Proc Natl Acad Sci USA **111:** 14607–14612

Soyano T, Kouchi H, Hirota A, Hayashi M (2013) NODULE INCEPTION directly targets NF-Y subunit genes to regulate

essential processes of root nodule development in *Lotus japonicus*. PLoS Genet **9:** e1003352

Soyano T, Shimoda Y, Hayashi M (2015) NODULE INCEPTION antagonistically regulates gene expression with nitrate in *Lotus japonicus*. Plant Cell Physiol **56:** 368–376

Streeter J, Wong PP (1988) Inhibition of legume nodule formation and N_2 fixation by nitrate. Crit Rev Plant Sci **7:** 1–23

Suzaki T, Kim CS, Takeda N, Szczyglowski K, Kawaguchi M (2013) *TRICOT* encodes an AMP1-related carboxypeptidase that regulates root nodule development and shoot apical meristem maintenance in *Lotus japonicus*. Development **140:** 353–361

Suzaki T, Takeda N, Nishida H, Hoshino M, Ito M, Misawa F, Handa Y, Miura K, Kawaguchi M (2019) *LACK OF SYMBIONT ACCOMMODATION* controls intracellular symbiont accommodation in root nodule and arbuscular mycorrhizal symbiosis in *Lotus japonicus*. PLoS Genet **15:** e1007865

Suzaki T, Yano K, Ito M, Umehara Y, Suganuma N, Kawaguchi M (2012) Positive and negative regulation of cortical cell division during root nodule development in *Lotus japonicus* is accompanied by auxin response. Development **139:** 3997–4006

Suzuki T, Kawai T, Takemura S, Nishiwaki M, Suzuki T, Nakamura K, Ishiguro S, Higashiyama T (2018) Development of the Mitsucal computer system to identify causal mutation with a high-throughput sequencer. Plant Reprod **31:** 117–128

Tabata R, Sumida K, Yoshii T, Ohyama K, Shinohara H, Matsubayashi Y (2014) Perception of root-derived peptides by shoot LRR-RKs mediates systemic N-demand signaling. Science **346:** 343–346

Valkov VT, Rogato A, Alves LM, Sol S, Noguero M, Léran S, Lacombe B, Chiurazzi M (2017) The nitrate transporter family protein LjNPF8.6 controls the N-fixing nodule activity. Plant Physiol **175:** 1269–1282

Valkov VT, Sol S, Rogato A, Chiurazzi M (2020) The functional characterization of *LjNRT2.4* indicates a novel, positive role of nitrate for an efficient nodule N_2-fixation activity. New Phytol **228:** 682–696

Vernié T, Kim J, Frances L, Ding Y, Sun J, Guan D, Niebel A, Gifford ML, de Carvalho-Niebel F, Oldroyd GED (2015) The NIN transcription factor coordinates diverse nodulation programs in different tissues of the *Medicago truncatula* root. Plant Cell **27:** 3410–3424

Wang Q, Huang Y, Ren Z, Zhang X, Ren J, Su J, Zhang C, Tian J, Yu Y, Gao GF, et al. (2020) Transfer cells mediate nitrate uptake to control root nodule symbiosis. Nat Plants **6:** 800–808

Wang R, Liu D, Crawford NM (1998) The *Arabidopsis* CHL1 protein plays a major role in high-affinity nitrate uptake. Proc Natl Acad Sci USA **95:** 15134–15139

Yendrek CR, Lee YC, Morris V, Liang Y, Pislariu CI, Burkart G, Meckfessel MH, Salehin M, Kessler H, Wessler H, et al. (2010) A putative transporter is essential for integrating nutrient and hormone signaling with lateral root growth and nodule development in *Medicago truncatula*. Plant J **62:** 100–112

Yoro E, Suzaki T, Toyokura K, Miyazawa H, Fukaki H, Kawaguchi M (2014) A positive regulator of nodule organogenesis, NODULE INCEPTION, acts as a negative regulator of rhizobial infection in *Lotus japonicus*. Plant Physiol **165:** 747–758